Accepted Manuscript

Design, synthesis and biological evaluation of small molecules as potent glucosidase inhibitors

Santanu Hati, Sanjay M. Madurkar, Chandramohan Bathula, Chiranjeevi Thulluri, Rahul Agarwal, Faiza Amber Siddiqui, Poonam Dangi, Uma Adepally, Ashutosh Singh, Shailja Singh, Subhabrata Sen

PII: S0223-5234(15)30016-7

DOI: 10.1016/j.ejmech.2015.04.059

Reference: EJMECH 7874

To appear in: *European Journal of Medicinal Chemistry*

Received Date: 5 December 2014

Revised Date: 23 April 2015

Accepted Date: 25 April 2015

Please cite this article as: S. Hati, S.M. Madurkar, C. Bathula, C. Thulluri, R. Agarwal, F.A. Siddiqui, P. Dangi, U. Adepally, A. Singh, S. Singh, S. Sen, Design, synthesis and biological evaluation of small molecules as potent glucosidase inhibitors, European Journal of Medicinal Chemistry (2015), doi: 10.1016/j.ejmech.2015.04.059.

Design, synthesis and biological evaluation of small molecules as potent glucosidase inhibitors

Santanu Hati,[1§] Sanjay M. Madurkar,[2§] Chandramohan Bathula,[1] Chiranjeevi Thulluri,[3] Rahul Agarwal,[4] Faiza Amber Siddiqui,[5] Poonam Dangi,[4] Uma Adepally,[3] Ashutosh Singh,[4] Shailja Singh*[4] and Subhabrata Sen*[2]

[1] Department of Chemistry, School of Natural Sciences, Shiv Nadar University, UP 201314, India

[2] Department of Chemistry, Mahatma Gandhi University, Ri Bhoi, Meghalaya, India

[3] Institute of Science, Jawaharlal Nehru Technical University, Kukatpally, Hyderabad, Telangana, India

[4] Department of Life Science, School of Natural Sciences, Shiv Nadar University, UO 201314, India

[5] International Centre for Genetic Engineering and Biotechnology, New Delhi, India

[§] Equal contributor

Abstract. Herein we have reported design, synthesis and *in vitro* biological evaluation of a library of bicyclic lactams that led to the discovery of compounds **6** and **7** as a novel class of α-glucosidase inhibitors. They inhibited α–glucosidase (yeast origin) in a mixed type of inhibition with an IC_{50} of ~150 nM. Molecular docking studies further substantiated screening results. Interestingly phenotypic screening of this library against the human malaria parasite revealed **7** as a potent antiplasmodial agent.

1. Introduction.

Diabetes mellitus is one of the most common non-communicable diseases of the globe.[1-2] The prevalence of diabetes is estimated to double by 2030 with 69% increase in developing countries and 20% increase among adults in developed countries. Despite phenomenal progress in medical science, diabetes continues to be a major killer.[3]

Diabetes is a disease characterized by chronic hyperglycemia that leads to development of macro and micro vascular complication. [4] Hence, one of the therapeutic approaches in type 2 diabetes is to reduce the demand for insulin by lowering the corresponding postprandial hyperglycemic levels via inhibition of enzymes in the digestive organs such as the α-glucosidases.[5] Research has

shown that inhibition of α-glucosidase enzyme located at the intestinal brush border of the intestine may play a role in the lowering of postprandial hyperglycemia.[5]

To date, the only reported inhibitors of glycosidase enzymes are either complex natural products, like Validoxylamine A, MDL 25637 (α-homonojirimycin-7-*O*-β-D-glucopyranoside), trehazolin, acarbose, nojirimycin, castanospermineetc., or synthetic analogs like DNJ, N-butyl-DNJ, DANA and others.[6] Iminosugars and thiosugar derivatives are also one of the most promising glycosidase inhibitors.[7] However there are not very many non-sugar synthetic compounds as potent glycosidase inhibitors.[8-15] Hence, discovery of such molecules will have a niche appeal and applicability in the pharmaceutical world.

Herein we report our investigation involving identification of a small molecule inhibitor of α-glucosidase *via* routine glucosidase profiling of small molecule libraries unbiased towards any specific targets. This exercise resulted in generating a potential hit compound **1** possessing bicyclic lactam motif. Design and synthesis of a focused library of bicyclic lactams around this motif with diverse functionalities followed by *in vitro* screening against yeast α-glucosidase enzyme generated **6** and **7** as most potent compounds with IC_{50} ~150 nM. Reaction kinetics suggested that they are mixed inhibitors.

In addition phenotypic screening against *3D7* strain of Plasmodium falciparum revealed decent antiplasmodial activity of **7**.

2. Results and discussion

2.1 Initial screening,

To begin with we subjected our in-house compound collection, unbiased towards any specific targets in a routine glycosidase panel profiling. The exercise resulted in generating **1** as an interesting hit molecule with IC_{50} of 2μM against yeast α-glucosidase. **1** was obtained by the dihydroxylation of the previously reported cyclic ene-lactam **2**.[16]

2.2 Library design and synthesis

In a bid to generate the library from **1** we envisioned **8,** the diastereomer of **1,** as a library member followed by 6-membered bicyclic lactams **9** and **10** as the higher homologs of **1**. Additionally, we choose **3** and **5** where oxygen is located differently than in **1**. Also included in

the library are the dehydroxylated analog **6** and the unsaturated analogs **7** and **2** (the immediate precursor of **1**). We further envisioned that epoxide analogs **4** and **11** will streamline the SAR, hence they were synthesized too (fig. 4). In a bid to diversify the aromatic moiety of the bicyclic lactams, benzyl and indoline substituted bicyclic lactams **12** and **13** were incorporated. Finally we envisioned a set of dimeric bicyclic lactams **14-17** in our library. By virtue of possessing diverse biological activity the dimeric compounds have lately gained lot of importance in the pharmaceutical world and that prompted their inclusion in this focused library (figure 1).

(**Figure 1)**

Synthesis of compounds **3**, **4**, **5** and **10** were accomplished following literature procedures.[17-19] Compound **2** was obtained from bicyclic lactam **18**, by phenyl selenium bromide mediated addition-reduction followed by oxidation of the arylselenium intermediate with hydrogen peroxide**. 18** in turn was obtained by condensing *S*-pyroglutaminol and benzaldehyde with catalytic *p*-toluenesulfonic acid (PTSA) in refluxing toluene. Dihydroxylation of **2** in presence of *N*-methylmorpholine-N-Oxide and osmium tetraoxide in 1:1 acetone: water afforded **1**. In a different reaction, epoxidation of **2** with meta-perbenzoic acid (mCPBA) resulted in **4**. In a similar effort compound **6** (synthesized from *R*-pyroglutaminol and benzaldehyde) was converted to **7**. And a similar dihydroxylation of **7** yielded **8**. Epoxidation of **7** provided **11**. Simple condensation of *S*-phenylalaninol and *S*-Tryptophanol with 2-(2-nitrophenyl)-4-oxopentanoic acid in toluene in catalytic *p*-toluene sulfonic acid furnished **12** and **13**. Finally oxidative homoenolate coupling of bicyclic lactams **5**, **18**, **19** and **20** in presence of lithium bis(trimethylsilyl)amide (2.1 eq.) and 2.1 eq. of the oxidant iodine (I_2) afforded **14-17**. The synthesis of the library was designed in a way where each member of the library can be obtained in minimum number of steps and with high steps/molecule ratio (~1.7), thereby making the library generation more facile (figure 2).

(**Figure 2**)

2.3 In vitro assay against α-glucosidase (yeast origin)

We screened all the compounds against α-glucosidase enzyme of yeast origin along with acarbose, a known α-glucosidase inhibitor, as the positive control. The percentage inhibition on the α-glucosidase was measured at a concentration of 10 µM to 50 µM

(refer *SI* for experimental details). To assess the potency of our compounds, the inhibitory activities were plotted against the concentrations using non-linear regression approach (sigmoid curves) (cf. *SI*) from which their IC_{50} values were computed (Table 1). Among the compounds screened, **6** and **7** exhibited strong inhibition against α-glucosidase with IC_{50}s of 0.17 and 0.15 μM respectively, faring much better than acarbose control (900nM). Compounds **2** and **8** also bind effectively with IC_{50} ranging between 0.19 & 0.21 μM. To further probe the inhibitory effect of our compounds, we obtained their dose responses against α-glucosidase. The results showed that the activity of α-glucosidase was reduced by majority of our compounds (**2**, **6**, **7** and **8**) in a dose-reliant fashion thereby indicating their strong affinity towards the enzyme (Figure 3).

(**Table 1**)

(**Figure 3)**

2.4 Molecular Docking and modelling

With the IC_{50} values in hand, we wanted to understand the binding interactions of the initial compound **1** and most active compounds **6** and **7** with α–glucosidase. This would enable us to design more active analogues of **1**. Even though the X-ray crystallographic structure of α-glucosidase has been reported for some bacteria, the three dimensional structural information is not available for the yeast α-glucosidase enzyme. Hence we constructed the 3D structure of α-glucosidase by homology modeling. The sequence of α-glucosidase was downloaded from Uniprot (ID: P10253). BLASTP ® against protein data bank was performed in order to identify the template for sequence alignment. Human Maltase-Glucoamylase (PDB ID: 2QLY, 3L4T) were showing good similarity to our query sequence.[20] Residues starting from 89 are aligning to these PDB and showing 44% identity. These two protein structures were therefore selected to model α-glucosidase using homology modelling. The homology model of α-glucosidase was built using Modeller v9.14. Three models were generated using Modeller v9.14 and the model having best DOPE score is selected for further studies.[21] The energy of the model was minimized using MOE energy minimization algorithm using Force Field MMFF94x. The stereochemical quality of this model was validated by the Ramachandran plot using the PROCHECK program. 98.1% residues are in the favored and allowed regions, only 1.9% are outliers and no active site residue lie in this outlier region. Further the model is also validated using verify 3D program (figure 3).

(**Figure 4**)

Molecular modelling of **1** revealed that it was bound deeply into the binding cavity of α-glucosidase and showed interaction with the residues Lys 609, Asp 724, Leu 613, Gln 688, Ile 726, Ala 610, Thr 725, Gln 575, Phe 579, Val 728 & Asp 686 residues. **1** was found to form a hydrogen bond with the δ-amino moiety of Lys 609 and carbonyl group of amide moiety of Asp 724 (figure 2).

(**Figure 5**)

Next both compounds **6** and **7** were docked against the protein (figure 6 and 7). **6** and **7** bind to the active site residues of modelled α-glucosidase protein by forming one hydrogen bond and few other non-bonded interactions. For **6,** the hydrogen bond is formed with Asp 686 residue while His 729, Asn 727, Val 728, Thr 725, Pro 722, Ile 726, Gln 688, Leu 719, Pro 720 residues shared non-bonded interactions. Similarly **7** binds to the active site residues of modelled α-glucosidase protein by the hydrogen bond formed with Asp 686 residue while Thr 725, Gln 688, His 729, Pro 722, Ile 726, Val 728, Asn 727, Leu 719, Pro 720 residues shared non-bonded interactions. **6** and **7** showed similar binding with the receptor but the energy of the docked model is different. **1** showed stronger binding as compared to **6** and **7** but the stability of docked model is better in case of **6** and **7**. This may be the reason why **6** and **7** demonstrated better activity than **1** (Figures 6a and b).

(**Figure 6a**)

(**Figure 6b**)

2.5 Reaction kinetics study

Enzyme kinetic assays were conducted with the most active compounds *viz.* **6** and **7** to understand their mode of inhibition to α-glucosidase. This was determined by employing primary (Lineweaver-Burke) and secondary plots of inhibition kinetics (Figures 7 [a] and [b]) for the compounds. As revealed from the Lineweaver-Burke plot, the data points of **6** and **7** intersected in the second quadrant thereby indicating a mixed type of inhibition.

The mixed inhibition is an intermediate of the competitive and uncompetitive inhibition and can be represented as shown in the equation below (eq. 1).

(**Equation 1**)

As mixed inhibitors, **6** and **7** were able to bind to either the free α-glucosidase (E) or the α-glucosidase-substrate (pNPG) complex (E+S). The two inhibition constants in the mixed inhibition, K_{ia} and K_{ib} signified the equilibrium constant of dissociation of the $I + E$ (inhibitor-enzyme) complex and the $I + ES$ (inhibitor-bound enzyme substrate) complex. These values for **6** and **7** were computed from the secondary plots of the slope and Y-intercept from the Lineweaver-Burke plot versus inhibitor concentration (refer to *SI*). K_{ia} and K_{ib} of **6** were determined to be 11.2µM & 17.5µM and those for **7** were 22.6µM & 33.7µM respectively. These constants show that both the compounds have strong potency to bind to the free enzyme.

(**Figure 7**)

2.5 Phenotypic screening against malaria phenotype (3D7).

Since α-glucosidase inhibitors possess versatile mode of action against multiple therapeutic areas (*viz.* cancer, viral infection, malaria and etc.) other than diabetes we subjected the library of compounds to a phenotypic screening against the malaria parasite, Compound **7** showed remarkable inhibition against *3D7* strain of *Plasmodium Falciparum*). The parasites were treated at the ring stage and the percent parasitemia was calculated at the trophozoite stage of the second cycle (i.e. after 72 hours of incubation). The percent inhibition of invasion was calculated *w.r.t* the untreated control and nearly 65% inhibition was observed in presence of **7** (figure 8).

(**Figure 8**)

The fact that the same compound **7** showed activity against α-glucosidase and *3D7* strain of malaria parasite forced us to rethink about any connection between α-glucosidase and malaria parasite life cycle. However this is a preliminary result. Perhaps there is a plausible connection between the two but no direct evidence for such an observation is evident yet. Much exhaustive investigation is required to connect diabetes and malaria. It is an interesting avenue to explore for

the medicinal chemists. Further work on this is ongoing in our lab.

3. Conclusion

Herein we have discussed design and synthesis of a focused library of compounds based on bicyclic lactam **1**. It was identified from a random unbiased screening of our in-house library. *In vitro* screening of the library against yeast α-glucosidase generated two novel inhibitors **6** and **7**, with IC_{50} in the range of 150 – 200 nM. Reaction kinetics indicated that both of them have mixed type inhibition against α-glucosidase. Molecular docking of **6** and **7** against the homology model of α-glucosidase rationalized their activity. Interestingly, phenotypic screening of the library yielded **7** as a potent inhibitor of *3D-7* strain of Malaria Parasite Plasmodium *Falciparum*. Both antiplasmodial and anti α-glucosidase property of the **7**, opens a possibility of development of this compound as a potential treatment option for both the diseases.

4. Materials and methods

General Experimental

Reagents were obtained from Aldrich Chemical (www.sigma-aldrich.com) or Acros Organics (www.fishersci.com) and used without further purification. Optima grade solvents were obtained from Fisher Scientific (www.fishersci.com), degassed with Argon, and purified on a solvent drying system as described, unless otherwise indicated. Lithium hexamethyl disilylamide (LHMDS) was obtained from Aldrich in SureSeal bottles. Phenyl selenium bromide was obtained from Acros. Compounds **6** and **3**-**5**, **9**-**11** and **18**-**20** are prepared from the literature procedure.[17-19] The single crystal X-Ray of **11a** (the amine compound from **11**), confirms the relative configuration of **11**. All reactions were performed in flame-dried glassware under positive Argon pressure with magnetic stirring unless otherwise noted. Rubber septa and syringes were used for the transfer of liquid reagents and solutions. Syringes were purged with argon prior to use. TLC was performed on 0.25 mm E. Merck silica gel 60 F254 plates and visualized under UV light (254 nm) or by staining with potassium permanganate ($KMnO_4$), phosphomolybdic acid (PMA), iodine (I_2), or *p*-anisaldehyde. Silica flash chromatography was performed on E. Merck 230-400 mesh silica gel 60. IR spectra were recorded on a Perkin Elmer Spectrum 100 FTIR spectrometer with peaks reported in cm-1. NMR spectra were recorded on Varian

400MR and Varian 300 instruments at 24°C in $CDCl_3$ unless otherwise indicated. Spectra were processed using VNMR J 3.2 software, and chemical shifts are expressed in ppm relative to TMS (^1H, 0 ppm) or solvent signals: $CDCl_3$ (^1H, 7.26; ^{13}C, 77.0 ppm); coupling constants are expressed in Hz. Mass spectra were obtained at the Shiv Nadar University Analytical Facility on an Agilent 6540QTOF by electrospray (ESI) ionization.

(3R,7aS)-3-phenyl-1,7a-dihydropyrrolo[1,2-c]oxazol-5(3H)-one (**2**).

To the solution of bicyclic lactam **18** (900mg, 1eq) in THF (9mL) was added 1M solution of LiHMDS in THF (8.8mL, 2eq) at -78°C, pale yellow solution was allowed to stir 30 min. After that solution of PhSeBr (1.15g, 1.1 eq.) in THF was added drop-wise over 10 minutes. Reaction mixture was further stirred for 30 min at -78°C. Reaction progress was monitored by TLC. Reaction mixture was quenched by adding saturated aqueous NH_4Cl solution, and then warmed to rt and extracted in diethyl ether (50 mL*3). The organic extracts were separated and concentrated to afford phenyl selenylated product.

Phenyl selenylated product dissolved in dichloromethane (40 mL) and treated with 30% H_2O_2 (6 eq.) at 0°C. The resulting heterogeneous mixture was allowed to warm to rt while stirring vigorously for 16 h. The aqueous phase was extracted with CH_2Cl_2, and the organic extracts were combined and washed successively with 1N HCl and saturated aqueous $NaHCO_3$. The organic phase was dried (Na_2SO_4) and concentrated under reduced pressure to afford a crude compound, which further purified by column chromatography (30% EA in *n*-Hexane) to afford alpha beta unsaturated compound **2** (600mg). ^1H NMR (300 MHz, DMSO-D_6): δ 7.57-7.35 (m, 7H), 6.18-6.17 (d, J = 5.2 Hz, 1H), 5.95 (s, 1H), 4.78-4.74 (t, J_1 = 7.6 Hz, J_2 = 15.6 Hz, 1H), 4.27-4.24 (t, J_1 = 7.2 Hz, J_2 = 15.2 Hz, 1H), 3.34-3.30 (m, 1H). ^{13}C NMR (75 MHz, DMSO-D_6) 176.95, 147.82, 138.51, 129.17, 128.61, 128.42, 126.13, 87.37, 68.04, 65.11 ppm. AQUITY UPLC (MS ESI): $[M + H]^+$ calcd for $C_{12}H_{11}NO_2$ 202.22, found 202.10

(3R,6R,7R,7aR)-6,7-dihydroxy-3-phenyltetrahydropyrrolo[1,2-c]oxazol-5(3H)-one (**1**).

Compound **2** (200 mg, 1 eq.) and 50% solution of acetone in water (4mL) purged with nitrogen and then it was charged with 50% aqueous N-methylmorpholine-N-oxide (NMO) (0.4mL) and 2% solution of OsO_4 in butanol (0.4mL) at 25°C. Reaction mixture was stirred for 16h at rt. Once TLC indicates complete consumption of starting material

the reaction mixture was quenched with aq. solution of Na_2SO_3. It was extracted with ethyl acetate (4 X 25mL), Organic layer dried over sodium sulphate and distilled off on rotary evaporator to afford white solid compound **1** (150mg). ^{1}H NMR (300 MHz, DMSO-D_6): δ7.40-7.34 (m, 5H), 6.08 (s, 1H), 5.88-5.87 (m, 1H), 5.52-5.38 (m, 1H), 4.27-4.22 (m, 1H), 4.08-3.96 (m, 3H), 3.95-3.66 (m, 1H). ^{13}C NMR (75 MHz, DMSO-D_6) 174.78, 137.22, 128.92, 128.58, 125.99, 110.01, 87.00, 74.23, 71.00, 69.24, 65.07 ppm. AQUITY UPLC (MS ESI): $[M + H]^+$ calcd for $C_{12}H_{13}NO_4$ 236.24, found 236.14. $[\alpha]^{20}_D$ +46.3 (c 1, CH_3OH)

(3S,7aR)-3-phenyl-1,7a-dihydropyrrolo[1,2-c]oxazol-5(3H)-one (**7**).

Reaction procedure is same as **2**, Reaction done on 800 mg scale from **8** to afford 500mg of desired compound (**7**). ^{1}H NMR (300 MHz, DMSO-D_6): δ7.61-7.59 (d, J = 8Hz, 2H), 7.41-7.28 (m, 3H), 7.26-7.19 (m, 1H), 6.19- 6.17 (m, 2H), 4.65-4.61 (t, J_1 = 7.2 Hz, J_2 = 15.2 Hz, 1H), 4.29-4.21 (dd, J_1 = 7.6 Hz, J2 = 17.2 Hz, 1H), 3.45-3.41 (t, J_1 = 8.4 Hz, J_2 = 16.8 Hz, 1H). ^{13}C NMR (75 MHz, DMSO-D_6) 176.94, 150.59, 139.07, 128.54, 128.33, 127.75, 126.39, 86.95, 67.88, 65.27 ppm. AQUITY UPLC (MS ESI): $[M + H]^+$ calcd for $C_{12}H_{11}NO_2$ 202.22, found 202.05

(3S,6S,7S,7aS)-6,7-dihydroxy-3-phenyltetrahydropyrrolo[1,2-c]oxazol-5(3H)-one (**8**).

Reaction procedure is same as **1**, reaction done on 230mg scale to afford 220mg of **8** to generate desired compound as white solid. ^{1}H NMR (300 MHz, DMSO-D_6): δ7.38-7.37 (m, 5H), 6.08 (s, 1H), 6.04-5.89 (m, 1H), 4.52-4.49 (m, 1H), 4.08-3.69 (m, 2H), 3.67-3.33 (m, 1H). ^{13}C NMR (75 MHz, DMSO-D_6) 175.55, 175.24, 138.94, 138.68, 128.58, 128.45, 128.37, 126.13, 86.29, 86.20, 74.82, 73.78, 71.01, 70.03, 69.22, 64.40, 64.18, 58.81ppm. AQUITY UPLC (MS ESI): $[M + H]^+$ calcd for $C_{12}H_{13}NO_4$ 236.24, found 236.0. $[\alpha]^{20}_D$ -40.3 (c 1, CH_3OH)

(3S,6R,7aR)-3-benzyl-7a-methyl-6-(2-nitrophenyl)tetrahydropyrrolo[2,1-b]oxazol-5(6H)-one (**12**).

2-(2-nitrophenyl)-4-oxopentanoic acid (12 g, 50.6 mmol), (S)-phenyl alaninol (7.3 g, 52 mmol) and PTSA (12 mg, cat) were dissolved in toluene (120 mL). The flask was equipped with a Dean-Stark trap, and the solution was heated to reflux. After 16 h the solution was cooled, washed with saturated aqueous $NaHCO_3$, dried, and concentrated. Purification by flash column chromatography on silica gel (hexane/EtOAc, 1:1) generated

the desired compound which was triturated with diethyl ether to afford **12** (7.4 g, 41.5%) as white solid. ^{1}H NMR (300 MHz, DMSO-D_6): δ 7.98-7.95 (d, J = 8.1 Hz ,1H),7.59-7.36 (m, 3H), 7.32-7.22 (m, 6H), 7.15-7.02 (m, 1H), 4.68-4.48 (m, 1H), 4.40-4.28 (m, 1H), 4.25-4.16 (t, J_1 = 8.7 Hz, J_2 = 18Hz, 1H) , 4.01-3.89 (m, 1H), 3.15-3.11(m, 1H), 2.88-2.72 (m, 2H), 2.49-2.41 (t, J = 12Hz, 1H), 1.55 (s, 3H). ^{13}C NMR (75 MHz, DMSO-D_6) 175.28, 149.58, 136.93, 133.24, 132.23, 131.44, 129.62, 129.32, 128.57, 128.35, 126.76, 126.54, 125.46, 125.15, 124.26, 122.67, 122.57, 120.47, 120.25, 119.95, 111.78, 111.38, 97.18, 55.89, 47.98, 44.36, 39.99, 27.72, 25.02 ppm. AQUITY UPLC (MS ESI): [M + H]$^+$ calcd for $C_{12}H_{13}NO_4$ 353.39, found 353.30. $[\alpha]^{20}_D$ +21.5 (c 1, CH_3OH)

(3R,6S,7aS)-3-((1H-indol-3-yl)methyl)-7a-methyl-6-(2-nitrophenyl)tetrahydropyrrolo[2,1-b]oxazol-5(6H)-one (**13**).

2-(2-nitrophenyl)-4-oxopentanoic acid (6 g, 25 mmol), (S)-tryptophanol (4.94 g, 26 mmol) and PTSA (12 mg, cat) were dissolved in toluene (120 mL). The flask was equipped with a Dean-Stark trap, and the solution was heated to reflux. After 16 h the solution was cooled, washed with saturated aqueous $NaHCO_3$, dried, and concentrated. Purification by flash column chromatography on silica gel (hexane/EtOAc, 1:1) generated the desired compound which was triturated with diethyl ether to afford **13** (3.4 g, 35%) as colourless solid. ^{1}H NMR (300 MHz, DMSO-D_6): δ 10.90 (s, 1H), 7.59-7.56 (m, 1H), 7.37-7.35 (d, J = 8Hz, 1H), 7.29-7.28 (d, J = 1.6Hz, 1H), 7.17-7.13 (m, 1H), 7.10-7.06 (m, 1H), 7.01-6.98 (t, J = 1.2Hz, 1H), 4.92 (s, 2H), 4.34-4.31 (m, 2H), 4.20-4.11 (m, 1H), 3.93-3.89 (m, 1H), 3.17-3.08 (m, 1H), 2.96-2.91 (m, 1H), 2.10-2.04 (m, 1H), 1.51 (s, 3H). AQUITY UPLC (MS ESI): [M + H]$^+$ calcd for $C_{22}H_{24}N_3O_4$ 392.42, found 392.78. $[\alpha]^{20}_D$ +11.3 (c 1, CH_3OH)

Procedure for the synthesis of dimeric bicyclic lactam **14**:

(3aR,3'aR,4aS,4'aS,9bR,9'bR)-3a,3'a-dimethyl-3,3a,3',3'a,4a,4'a,5,5'-octahydro-1H,1'H-[2,2'-biindeno[1,2-d]pyrrolo[2,1-b]oxazole]-1,1'(2H,2'H,9bH,9'bH)-dione (**14**).

To a solution of bicyclic lactam **19** (10.0 g, 43.6 mmole) in THF (100 ml) was added LiHMDS (1.0 M solution in THF, 47.97 ml, 47.97 mmole) at -78°C in a drop wise manner. The reaction mixture was stirred for 30 min at that temperature. A solution of

iodine (11.07g, 43.6 mmole) in THF(10 ml) was added to the reaction mixture in drop wise manner over a period of 30 min. The reaction mixture was further stirred for 2 hours at -78°C and the warmed upto room temperature. Reaction progress was monitored by thin layer chromatography [eluent: 30% EA in *n*-hexane]. After completion of the reaction, the reaction mixture was cooled to -78°C and quenched by saturated ammonium chloride solution. The crude product was extracted in ethyl acetate (200 ml*2). Organic layer was washed with aqueous sodium thiosulphate. $5H_2O$ solution (250 ml), water (250 ml) and brine solution (250 ml). And then dried over sodium sulphate and distilled off on a rotary evaporator to afford the crude solid which was further purified by column chromatography (silica:100-200 mesh, eluent: 16% ethyl acetate in *n*-hexane) to afford off white solid compound (9.5 g, 47.7%). ^{1}H NMR (300 MHz, DMSO-D_6): δ 7.41-7.31 (t, *J* = 8Hz, 1H), 7.29-7.23 (m, 4H), 5.68-5.66 (d, *J* = 8Hz, 1H), 4.92-4.89 (m, 1H), 3.49-3.45 (m, 1H), 3.28-3.14 (m, 2H), 2.33-2.28 (m, 1H), 2.11-1.60 (m, 1H), 1.03 (s, 3H). ^{13}C NMR (75 MHz, DMSO-D_6) 179.2, 131.2, 130.4, 130.2, 126.6, 125.8, 72.1, 58.5, 52.3, 46.4, 42.8, 21.2 ppm. AQUITY UPLC (MS ESI): $[M + H]^+$ calcd for $C_{28}H_{28}N_2O_4$ 457.53, found 457.2. $[\alpha]^{20}_D$ +34.8 (c 1, CH_3OH).

(3R,3'R)-3,3'-diphenyloctahydro-[6,6'-bipyrrolo[2,1-b]oxazole]-5,5'(6H,6'H)-dione (**15**).

The above procedure was followed with bicyclic lactam **5** (0.5g, 2.46mmol), 1M LiHMDS (2.75mL), I_2 (0.63g, 2.46 mmol) and THF (10mL). ^{1}H NMR (300 MHz, $CDCl_3$): δ 7.38-7.28 (m, 10H), 5.31-5.30 (m, 2H), 5.29-5.08 (m, 2H), 4.60-4.56 (m, 2H), 3.87-3.83 (m, 2H), 3.64-3.59 (m, 1H), 2.68-2.60 (m, 2H), 1.99-1.92 (m, 2H). ^{13}C NMR (75 MHz, $CDCl_3$) 181.2, 128.2, 126.4, 126.3, 124.2, 67.3, 62.8, 61.9, 60.4, 42.1, 40.1, 28.1, 24.2 ppm. AQUITY UPLC (MS ESI): $[M + H]^+$ calcd for $C_{24}H_{24}N_2O_4$ 405.46, found 405.0.

(3R,3'R,7aR,7'aR)-7a,7'a-dimethyl-3,3'-diphenyloctahydro-[6,6'-bipyrrolo[2,1-b]oxazole]-5,5'(6H,6'H)-dione (**16**)

The above procedure was followed with bicyclic lactam **20** (0.5g, 2.30mmol), 1M LiHMDS (2.75mL), I_2 (0.6g, 2.30 mmol) and THF (10mL). ^{1}H NMR (300 MHz, $CDCl_3$):

δ 7.37-7.33 (t, *J* = 8Hz, 2H), 7.29-7.24 (m, 2H), 5.14-5.11 (t, *J* = 8Hz, 15.2Hz, 1H), 4.62-4.57 (t, *J* = 8.4 Hz, 16.8Hz, 1H), 4.11-4.07 (t, *J* = 7.2 Hz, 16Hz, 1H), 3.70-3.66 (t, *J* = 8.8 Hz, 17.6Hz, 1H), 2.45-2.40 (m, 1H), 2.21-2.15 (m, 1H), 1.49 (s, 3H). ^{13}C NMR (75 MHz, $CDCl_3$). AQUITY UPLC (MS ESI): $[M + H]^+$ calcd for $C_{26}H_{28}N_2O_4$ 433.5, found 433.0.

(3S,3'S)-3,3'-diphenyloctahydro-[6,6'-bipyrrolo[1,2-c]oxazole]-5,5'(3H,3'H)-dione (**17**)

The above procedure was followed with bicyclic lactam **18** (0.5g, 2.46mmol), 1M LiHMDS (2.75mL), I_2 (0.63g, 2.46 mmol) and THF (10mL). ^{1}H NMR (300 MHz, $CDCl_3$): δ 7.50-7.26 (m, 10H), 6.36 (s, 2H), 4.39-4.36 (m, 2H), 4.19-4.16 (m, 2H), 3.41-3.40 (m, 4H), 3.39-3.25 (m, 2H). ^{13}C NMR (75 MHz, $CDCl_3$). AQUITY UPLC (MS ESI): $[M + H]^+$ calcd for $C_{26}H_{28}N_2O_4$ 405.46, found 405.1.

***In vitro* assay of α-Glucosidase inhibitory activity**

The inhibitory potency of the compounds against α-glucosidase activity was assessed in 96-well plates using PNPG (4-nitrophenyl α-D-glucopyranoside) as a substrate according to the procedure reported by Ferreres et al.[22] Prior to screen, all the test compounds were solubilized in a suitable solvent, Dimethylsulfoxide (DMSO) and eventually diluted to attain the desired concentration. Briefly, each well was comprised of 100µL of substrate (2mM, PNPG dissolved in 2mM phosphate buffer at a pH of 7.2) and different test concentrations (10-100 µM). Then the final volume of the reaction mixture was made up to 200µl with 2mM phosphate buffer (pH 7.2). The hydrolytic reaction was commenced by the addition of α-glucosidase enzyme (0.5 IU/mL) (obtained from Sigma Aldrich, Bangalore) and the plates were incubated at 37°C for 15 min. The reaction was terminated by the addition of 50µL of 2N Na_2CO_3 solution. The absorbance was measured spectrophotometrically at 400 nm (Epoch reader; version 2.00.18). The decrease/increase in absorbance (ΔA) was compared with that of control (buffer instead of test compound) to compute the inhibitory profile of enzyme. The data used for the determination of IC50 concentrations were fitted by non-linear regression fitting and the variance analysis was carried out by using MINITAB 15 software (trail version). The concentration of inhibition required for 50% of α-glucosidase activity under the assay conditions was defined as the IC50 value. The half maximal inhibitory (IC_{50}) concentrations were determined from two independent

assays, performed in duplicate. Acarbose, an eminent α-glucosidase inhibitor, was employed as a positive control.

$$\text{Inhibition (\%)} = \Delta A_{control} - \Delta A_{sample} / \Delta A_{control} \times 100\%$$

One unit (IU) is defined as the amount of enzyme (α-glucosidase) which produces 1 μmol of PNP (*p*-nitro phenol) per min at 37°C and pH 7.2 under the conditions described above.

Inhibition-kinetic studies

The kinetic mode of inhibition of selected active compounds against α-glucosidase was determined as said above by preparing a series of test solutions in which the concentration of the substrate (PNPG) was varied in the presence of different concentrations of the inhibitors (10μM-100μM). The mode of inhibition (i.e. competitive, non-competitive, uncompetitive or mixed-type) of the test compounds was evaluated on the basis of the inhibitory effects on Km (dissociation constant) and V_{max} (maximum reaction velocity) of the enzyme.[23] This was determined using the primary (Lineweaver-Burke plot) plot, which is the double reciprocal plot of enzyme reaction velocity (V) versus substrate (pNPG) concentration (1/V versus 1/[pNPG]). Analysis of the same data by secondary plots of slope versus [Inhibitor] and Y-intercept versus [Inhibitor] were also performed. The Lineweaver-Burke equation follows as,

$$\frac{1}{v} = \frac{1}{V_{max}} + \frac{K_m}{V_{max}} \times \frac{1}{[S]}$$

Malaria-growth inhibition assays (GIA):

P. falciparum culture 3D7 was maintained in vitro at pH 7.4 in plastic petri-dishes using human O^+ erythrocytes, at 4% hematocrit, in RPMI-HEPES medium supplemented with 5% Albumanx, 50 μg/ml hypoxanthine, 25 mM NaHCO3 and 20 μg/ml gentamicin maintained in an atmosphere of 1% O2, 4% CO2, and 95% N2 at 37°C, as previously described (Ref).[24] Parasite cultures were synchronized using the sorbitol treatment. The GIA was put at ring stage at 0.3% parasitemia and 2% hematocrit in 96-well plates that were incubated in a sealed, humidified, gassed box. The assay plate was read after 72 hours i.e., at the trophozoite stage of the second cycle of invasion. 10 compounds were tested at two different concentrations of 10 μM and 50 μM in the GIAs. Parasitemia was determined using flow cytometry. For flow cytometry, 100 μl of 10-μg/ml ethidium bromide in phosphate-buffered saline (PBS; pH 7.3) was added to each well and incubated for 1 h in dark at room temperature. After centrifugation, the supernatant was discarded, cells were washed with PBS and re-suspended in 200 μl/well of PBS, and the samples

were processed using a FACS Calibar flow cytometer (Becton Dickinson, Franklin Lakes, NJ). Parasitemia was evaluated using FlowJo software (Tree Star, Inc., Ashland, OR) by first gating for intact erythrocytes by side scatter and forward scatter parameters and subsequently determining the proportion of ethidium bromide-positive cells indicating the percent parasitemia. All compounds were tested in duplicate.

5. Acknowledgement

We thank Shiv Nadar University for the support

6. References

1. A. E. Kitabchi, G. E. Umpierrez, J. M. Miles, J. N. Fisher, Hyperglycemic crises in adult patients with diabetes. Diabetes Care 32 (2009) 1335–1343.
2. E. Worrall E, S. Basu, K. Hanson, "Is malaria a disease of poverty? A review of the literature". Tropical Health and Medicine 10 (2005) 1047–59.
3. Diabetes Fact sheet N°312". WHO. October 2013. Retrieved 25 March 2014.
4. A. Qaseem A, S. Vijan, V. Snow, J. T. Cross, K. B. Weiss, D. K. Owens, Clinical Efficacy Assessment Subcommittee of the American College of Physicians Glycemic control and type 2 diabetes mellitus: the optimal hemoglobin A1c targets. A guidance statement from the American College of Physicians. Annals of Internal Medicine **147** (2007): 417–22.
5. S. A. Ross, E. A. Gulve, M. Wang, Chemistry and biochemistry of type 2 diabetes, Chem. Rev. 104 (2004) 1255e1282
6. N. Asano, Glycosidase inhibitors: update and perspectives on practical use, Glycobiology 13 (2003) 93R-104R.
7. N. Asano, Sugar-mimicking glycosidase inhibitors: bioactivity and application, Cell. Mol. Life Sci. 66 (2009) 1479-1492.
8. L. Gai-Li, H. Jia-Yun, Z. Aiqin, W. Yiqian, B. Wang, C. Wen-Hua, Toward potent a-glucosidase inhibitors based on xanthones: A closer look into the structure activity correlations, European Journal of Medicinal Chemistry, 46 (2011) 4050-4055.
9. Y. Chinthala, A. K. Domatti, A. Sarfaraz, S. P. Singh, N. K. Arigari, N. Gupta, S. K.V.N. Satya, J. K. Kumar, F. Khan, A. K. Tiwari, G. Paramjit, Synthesis, biological evaluation

and molecular modeling studies of some novel thiazolidinediones with triazole ring, European Journal of Medicinal Chemistry, 70 (2013) 308-314.

10. S. Wang, J. Yan, X. Wang, Z. Yang, F. Lin, T. Zhang, Synthesis and evaluation of the α-glucosidase inhibitory activity of 3-[4-(phenylsulfonamido)benzoyl]-2H-1-benzopyran-2-one derivatives, European Journal of Medicinal Chemistry, 45 (2010) 1250-1255.
11. T. Dendup, V. Prachyawarakom, A. Pansanit, C. Mahidol. S. Ruchirawat, P. Kittakoop, α-glucosidase inhibitory activitivities of isoflavanones, isoiflavones and pterocarpans from Mucuna pruriens, Planta Medica, 80, (2014), 604-608.
12. K. Takao, R. Ishikawa, Y. Sugita, Chemical and Pharmaceutical Bulletin, 62 (2014), 810-815.
13. H. Kashtoh, S. Hussein, A. Khan, S. M. Saad, J. A. J. Khan, M. K. Khan, S. Perveen, M. I. Choudhary, Bioorganic and Medicinal Chemistry 22 (2014), 5454-5465.
14. S. M. Saad, K. Javaid, I. Fatima, U. Salar, K. M. Khan, S. Perveen, M. I. Choudhary, 2-arylquinazolin-4(3H)-ones: A new class of α-glucosidase inhibitors, Bioorganic and Medicinal Chemistry (2014) ahead of print.
15. T. Damsud, S. Adisakwattana, P. Phuwapraisirisan, Three new phenylpropanoyl amides from the leaves of *Piper sarmentosum* and their α-glucosidase inhibitory activities. Phytochemistry Letters, 6 (2013), 350-354.
16. Y. Hamada, A. Kawai, Y. Kohno, O. Hara, T. Shioiri, New methods and reagents in organic. 83. Stereoselective total synthesis of AI-77-B, a gastroprotective substance from Bacillus pumilus AI-77. J. Am. Chem. Soc. 111 (1989) 1524-1525.
17. S. Sen, V. R. Potti, R. Surakanti, Y. L. N. Murthy, R. Pallepogu, Enantioselective synthesis of spirooxindoles via chiral auxiliary (bicyclic lactam) controlled S_NAr reactions, Organic & Biomolecular Chemistry 9, (2011), 358-360.
18. M. Amat, O. Lozano, C. Escolano, E. Molins, J. Bosch, Enantioselective Synthesis of 3,3-Disubstituted Piperidine Derivatives by Enolate Dialkylation of Phenylglycinol-Derived Oxazolopiperidone Lactams, J. Org. Chem., 72, (2007) 7756-7763.
19. N. Langlois, Diastereospecific formal synthesis of (2R,3S)-2-amino-tetradeca-5,7-dien-3-ol isolated from Xestospongia sp. Tetrahedron Letters, 42 (2001) 5709-5711.
20. R.L. Guerreiro, E. Carreiro, L. Fernandes, T. Cardote, R. Moreira, A.T. Caldeira, R. Guedes, A.J. Burke, Bioorganic & Med Chem. 21, (2013), 1911-1917.

21. E. P. Carreiro, P. Louro, G. Adriano, R.N. Vannuchi, R. Guedes, A.R. Costa, C. M.M. Antunes, R. C. Guedes, A.J. Burke, Bioorg. Chem. 54 (2014), 81-88.
22. M. I. Gil, F. Ferreres, F. A. Tomás-Barberán, Effect of Modified Atmosphere Packaging on the Flavonoids and Vitamin C Content of Minimally Processed Swiss Chard (*Beta vulgaris* Subspecies *cycla*) J. Agricultural and Food Chem., 46 (1998) 2007-2012
23. Benjamin T. Burlingham and Theodore S. Widlanski, An intuitive look at the relationship of Ki and IC_{50}: A More General Use for the Dixon Plot, Journal of Chemical Education 80 (2003) 214.
24. W. Trager, J. B. Jensen, Human malaria parasites in continuous culture. Science 193 (1976) 673–675.

7. Figure Captions

Figure 1. The library of bicyclic lactams designed around **1**

Figure 2. The synthetic scheme to access the small molecules depicted in the design (figure 1)

Table. 1. The *in vitro* activity of the library of pyrrolidines against yeast α-glucosidase

Figure 3. Inhibition of α-glucosidase enzyme activity as a function of inhibitors (from 10 μM to 50 μM) with Acarbose, as a reference standard

Figure 4. Ramachandran plot of the modelled α-glucosidase enzyme

Figure 5. Predicted binding mode of **1** in modelled α-glucosidase enzyme

Figure 6a. Predicted binding mode of **6** in modelled α-glucosidase enzyme

Figure 6b. Predicted binding mode of **7** in modelled α-glucosidase enzyme

Equation 1. Mixed inhibition

Figure 7. Double-reciprocal (Lineweaver-Burke) plot of the inhibition kinetics of α-glucosidase by compound **6 (A)** and **7 (B)**; α-Glucosidase (activity 0.5IU/mL) was subjected with compound **6** & **7** at 37°C for 10min, followed by varying concentrations of 4-nitrophenyl α-D-glucopyranoside (PNPG). IU: Defined as the amount of enzyme (α-glucosidase) which produces 1 μmol of PNP (p-nitrophenol) per minute at 37°C and pH under the conditions described in *SI*.

Figure 8. Malaria parasite growth inhibition assay

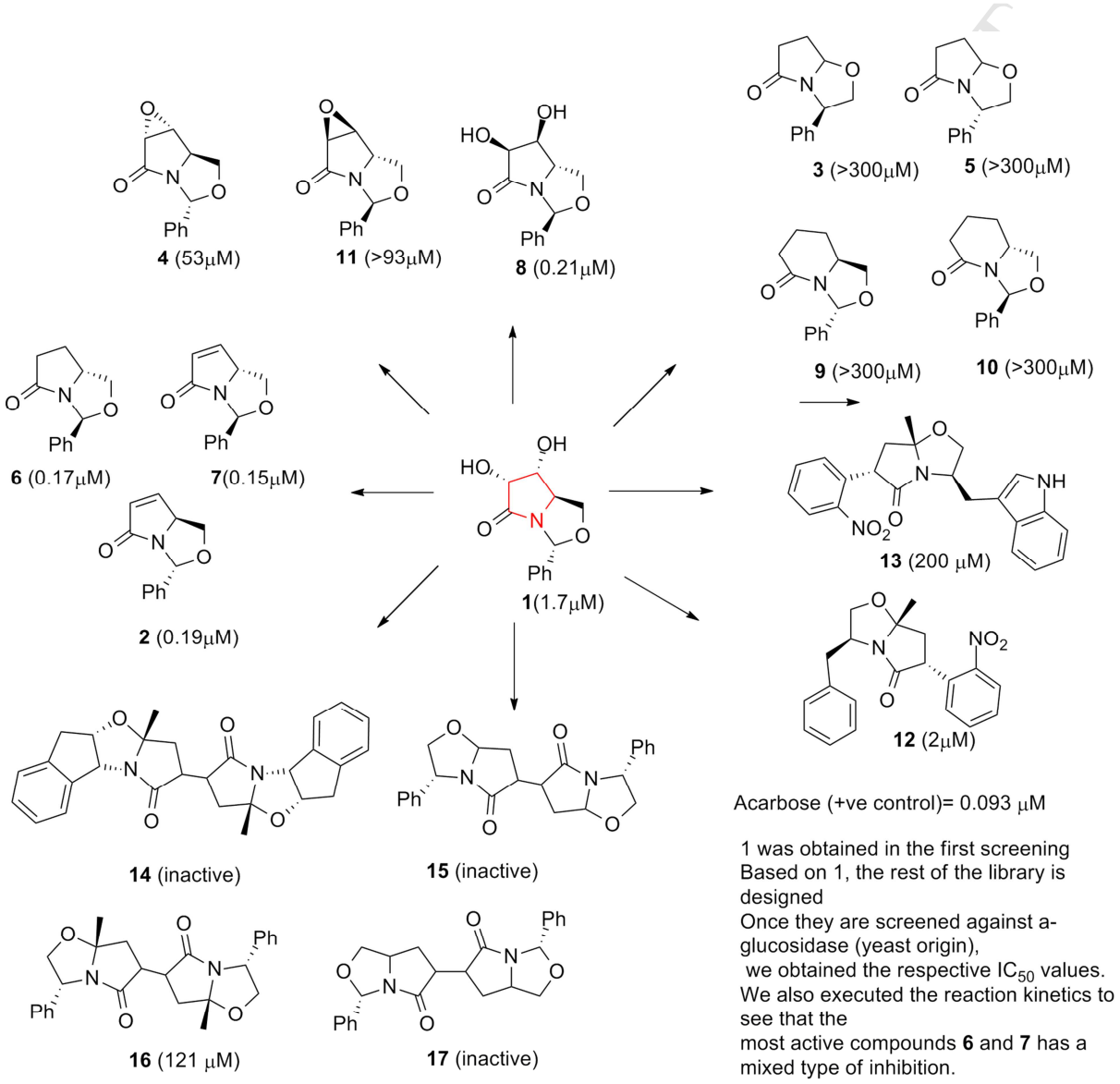

Figure 1. The library of bicyclic lactams designed around **1**

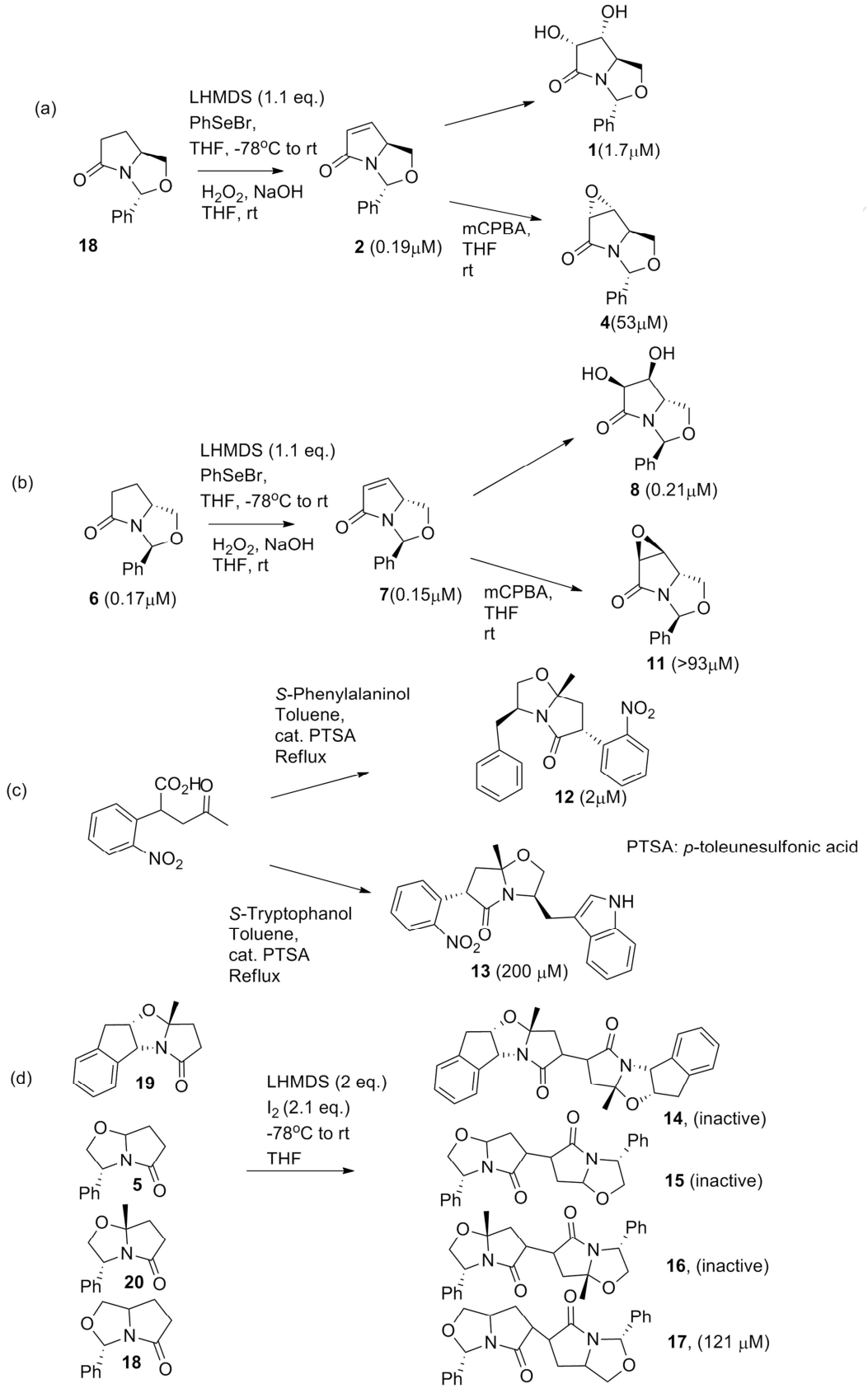
(a)
LHMDS (1.1 eq.)
PhSeBr,
THF, -78°C to rt
H2O2, NaOH
THF, rt
18
2 (0.19μM)
mCPBA,
THF
rt
1(1.7μM)
4(53μM)
(b)
LHMDS (1.1 eq.)
PhSeBr,
THF, -78°C to rt
H2O2, NaOH
THF, rt
6 (0.17μM)
7(0.15μM)
mCPBA,
THF
rt
8 (0.21μM)
11 (>93μM)
(c)
S-Phenylalaninol
Toluene,
cat. PTSA
Reflux
12 (2μM)
PTSA: p-toleunesulfonic acid
S-Tryptophanol
Toluene,
cat. PTSA
Reflux
13 (200 μM)
(d)
19
5
20
18
LHMDS (2 eq.)
I2 (2.1 eq.)
-78°C to rt
THF
14, (inactive)
15 (inactive)
16, (inactive)
17, (121 μM)

Figure 2. The synthetic scheme to access the small molecules depicted in the design (figure 1)

Table. 1. The *in vitro* activity of the library of pyrrolidines against yeast α-glucosidase

Entry	Compound	α-glucosidase (yeast) [a]IC_{50} (µmol)
1	**2**	0.19
2	**3**[c]	-
3	**4**	53
4	**5**[c]	-
5	**6**	0.17
6	**7**	0.15
7	**8**	0.21
8	**9**[c]	-
9	**1**	1.70
10	**10**[c]	-
11	**11**	95
13	**12**	-
14	**13**	213
15	**14**	-
16	**15**	-
17	**16**	-
18	**17**	121
19	**Acarbose**	0.093[b]

[a]Concentration of compound that reduced enzyme activity by 50% in an Activity (The values furnished were the means of two independents)
[b] The concentration was observed in our laboratory assay method
[c] > 50□ 50 concentration was observed in our laboratory

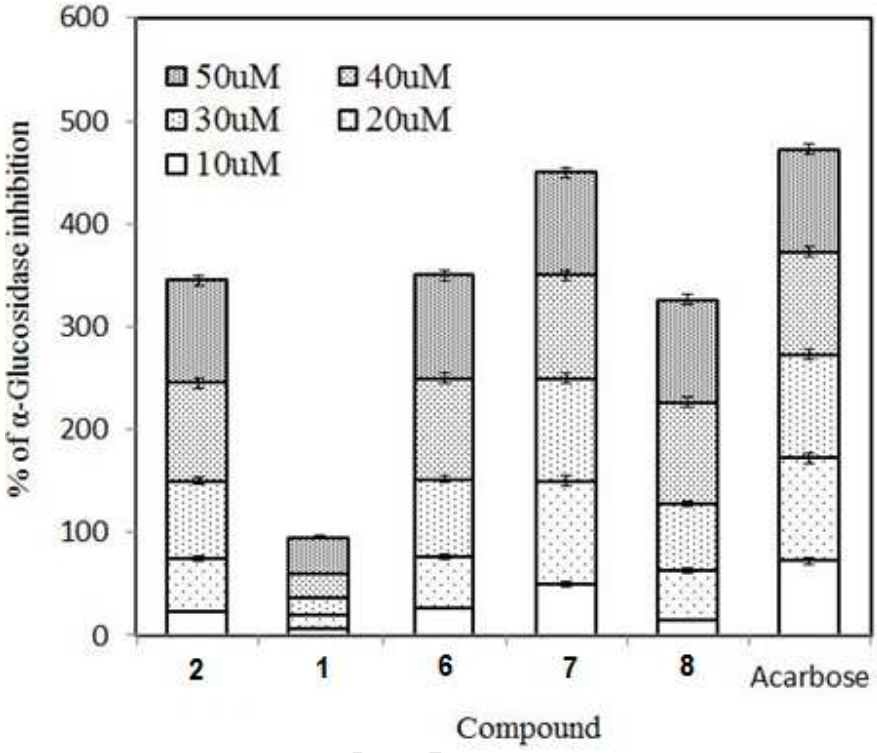

Figure 3. Inhibition of α-glucosidase enzyme activity as a function of inhibitors (from 10 μM to 50 μM) with Acarbose, as a reference standard

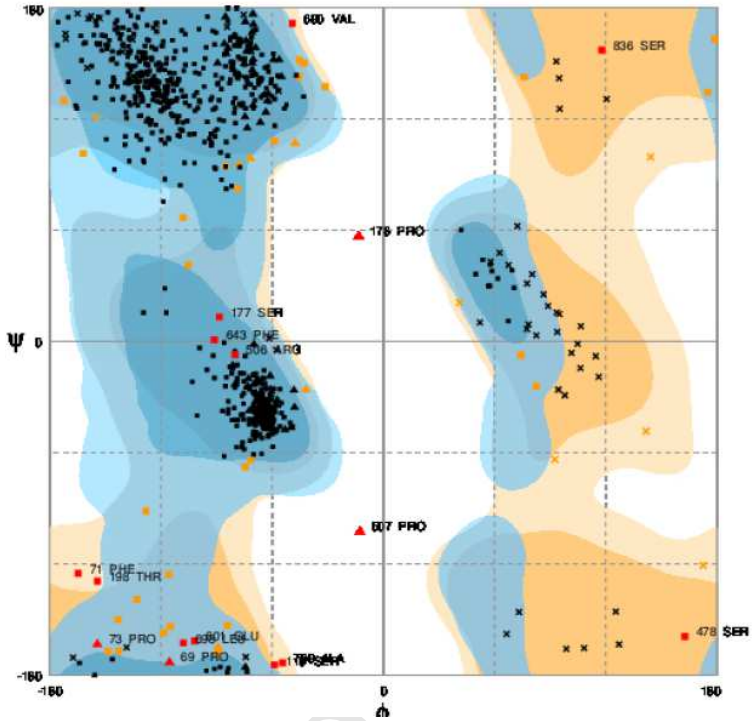

Figure 4. Ramachandran Plot of our α-glucosidase homology model

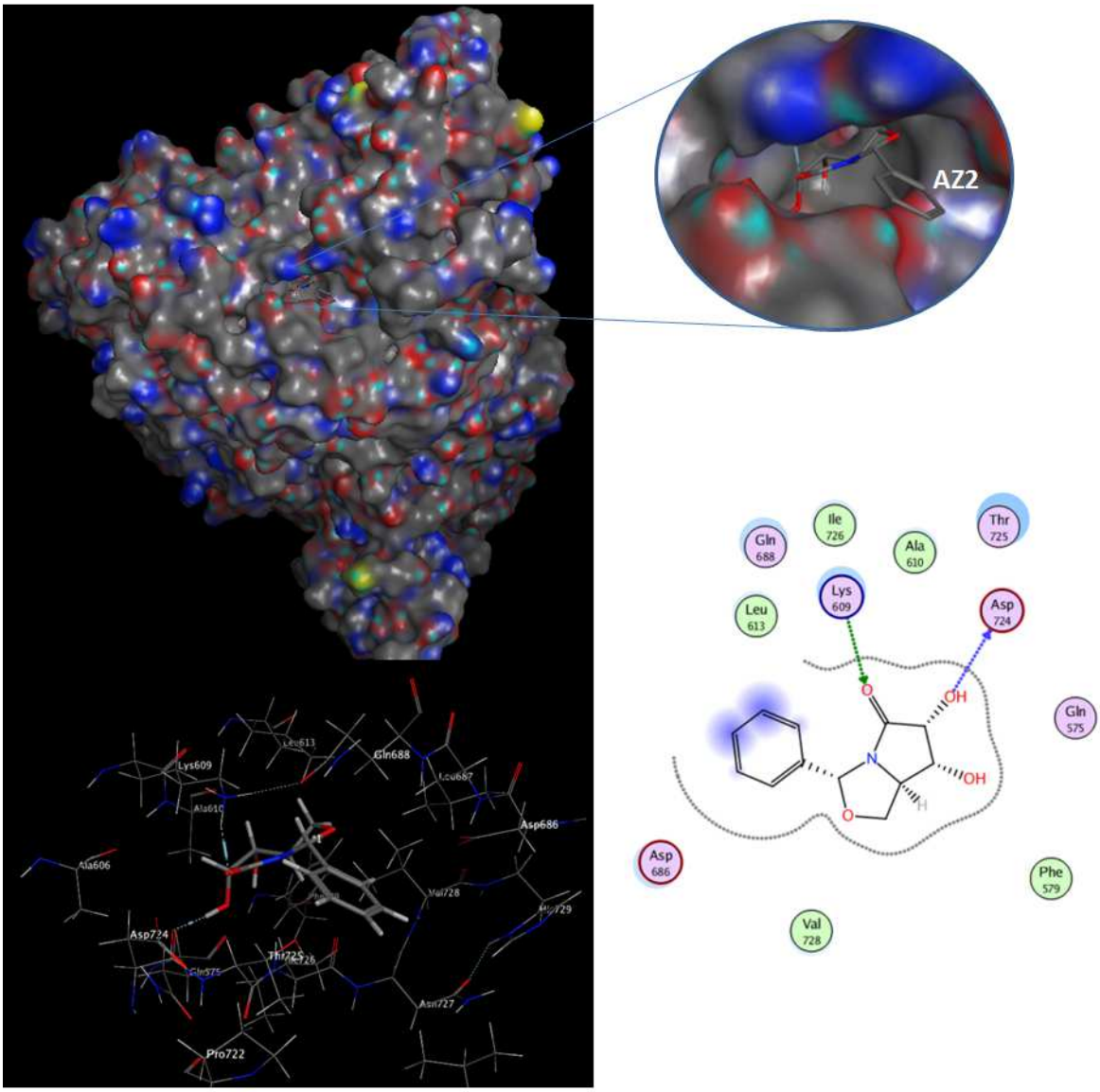

Figure 5. Predicted binding mode of **1** in modeled protein in a 3D representation along with 2D representation

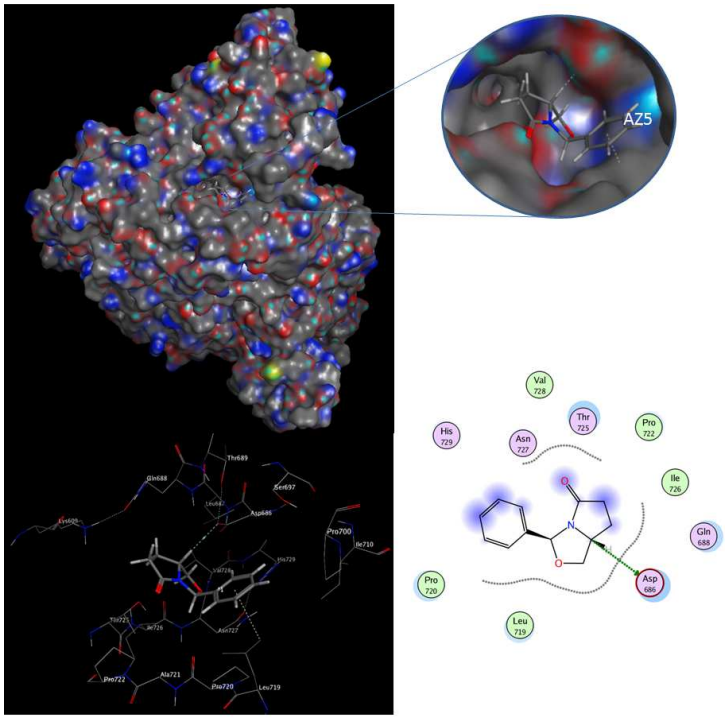

Figure 6a. Predicted binding mode of **6** in modelled protein

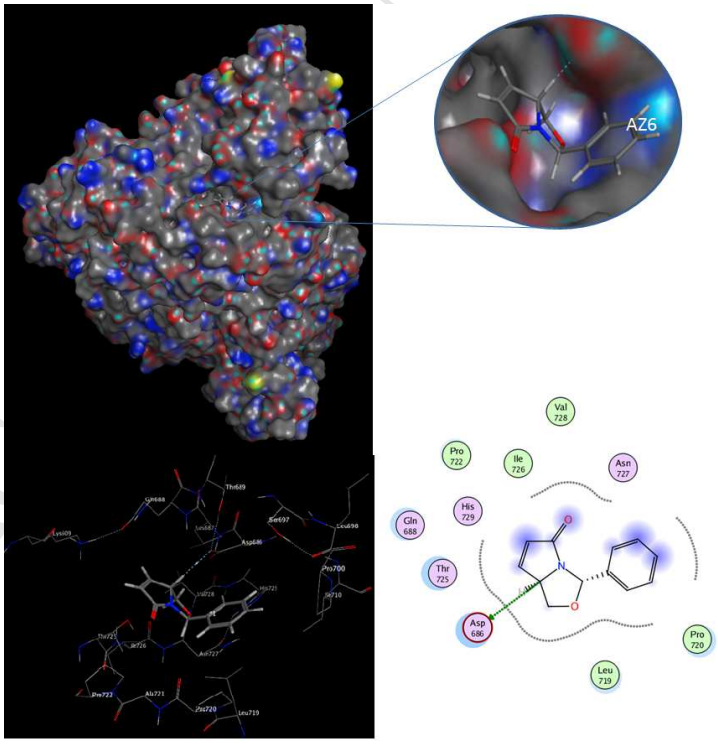

Figure 6b. Predicted binding mode of **7** in modelled protein

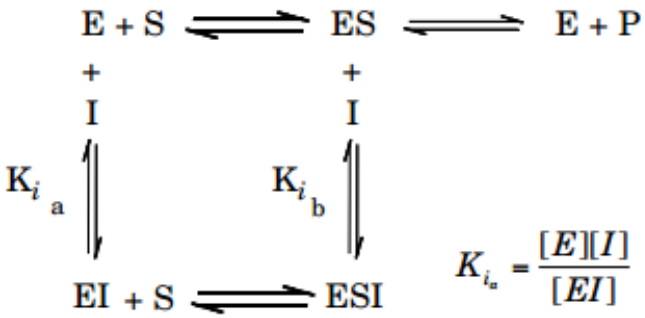

Equation 1. Mixed inhibition

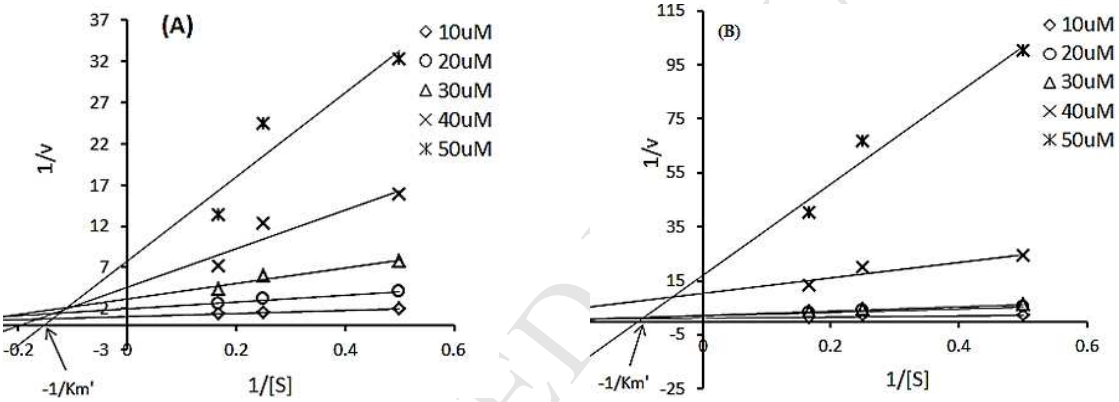

Figure 7. Double-reciprocal (Lineweaver-Burke) plot of the inhibition kinetics of α-glucosidase by compound **6 (A)** and **7 (B)**; α-Glucosidase (activity 0.5IU/mL) was subjected with compound **6** & **7** at 37°C for 10min, followed by varying concentrations of 4-nitrophenyl α-D-glucopyranoside (PNPG). IU: Defined as the amount of enzyme (α-glucosidase) which produces 1 μmol of PNP (p-nitrophenol) per minute at 37°C and pH under the conditions described in *SI*.

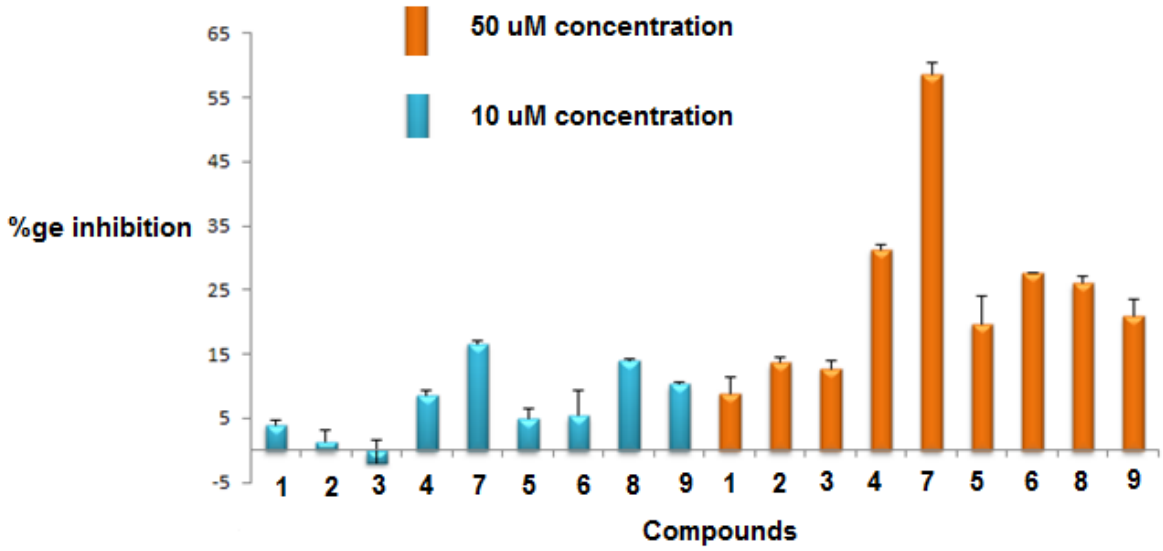

Figure 8. Malaria parasite growth inhibition assay

Graphical Abstract

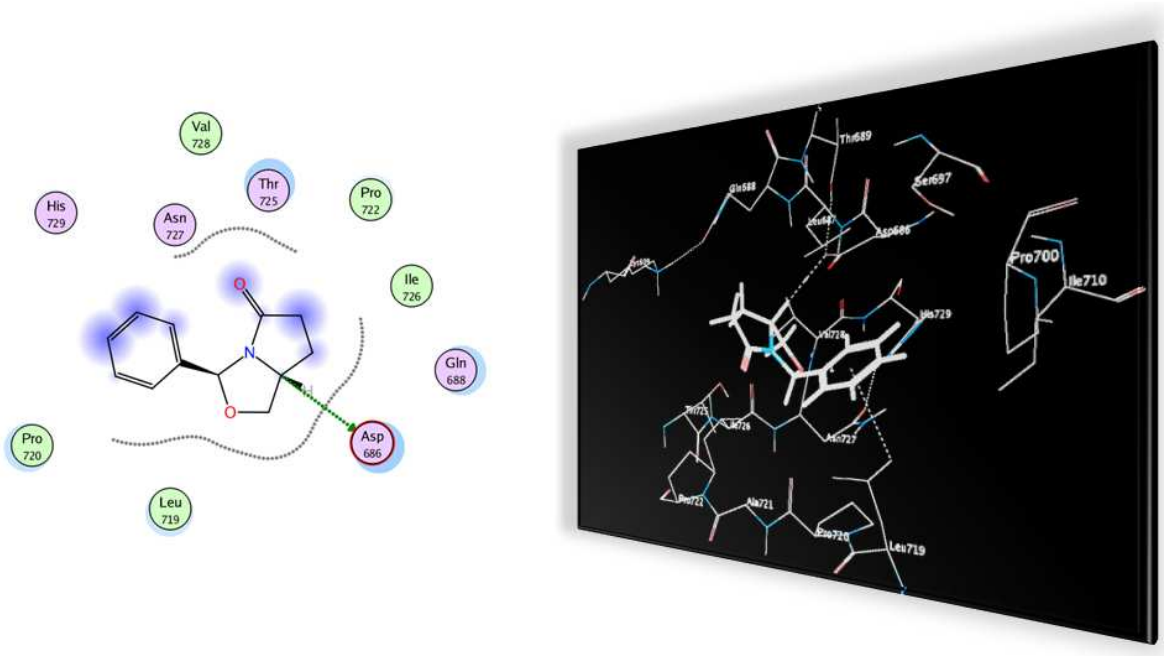

A bicyclic lactam has been discovered as a novel mixed inhibitor of α-glucosidase (yeast) enzyme that also inhibits 3D-7 strain of *Plasmodium Falciparum*.

Highlights

- We executed virtual screening of a library against a homology model of α-glucosidase.
- We designed and synthesized a molecular library.
- *In vitro* screening identified two compounds as potent α-glucosidase inhibitors
- Reaction kinetics suggested mixed type inhibition.
- Phenotypic screening of one of the compounds also indicated antimalarial properties

Design, synthesis and biological evaluation of small molecules as potent glycosidase inhibitors and antimalarials

Analysis of novel compounds

Sanjay M. Madurkar,[1] Santanu Hati,[5] Chandramohan Bathula,[5] Chiranjeevi Thulluri,[2] Rahul Agarwal,[3] Faiza Baig,[4] Poonam Dangi,[3] Uma Adepally,[2] Ashutosh Singh,[3] Shailja Singh[3] and Subhabrata Sen*[5]

[1] Department of Chemistry, Mahatma Gandhi University, Ri Bhoi, Meghalaya, India

[2] Institute of Science, Jawaharlal Nehru Technical University, Kukatpally, Hyderabad, Telengana, India

[3] Department of Life Science, Shiv Nadar University, PO Shiv Nadar University, Uttar Pradesh, India

[4] International Centre for Genomics Engineering and Biotechnology, New Delhi, India

[5] Department of Chemistry, Shiv Nadar University, PO Shiv Nadar University, Uttar Pradesh, India

Compound **2**

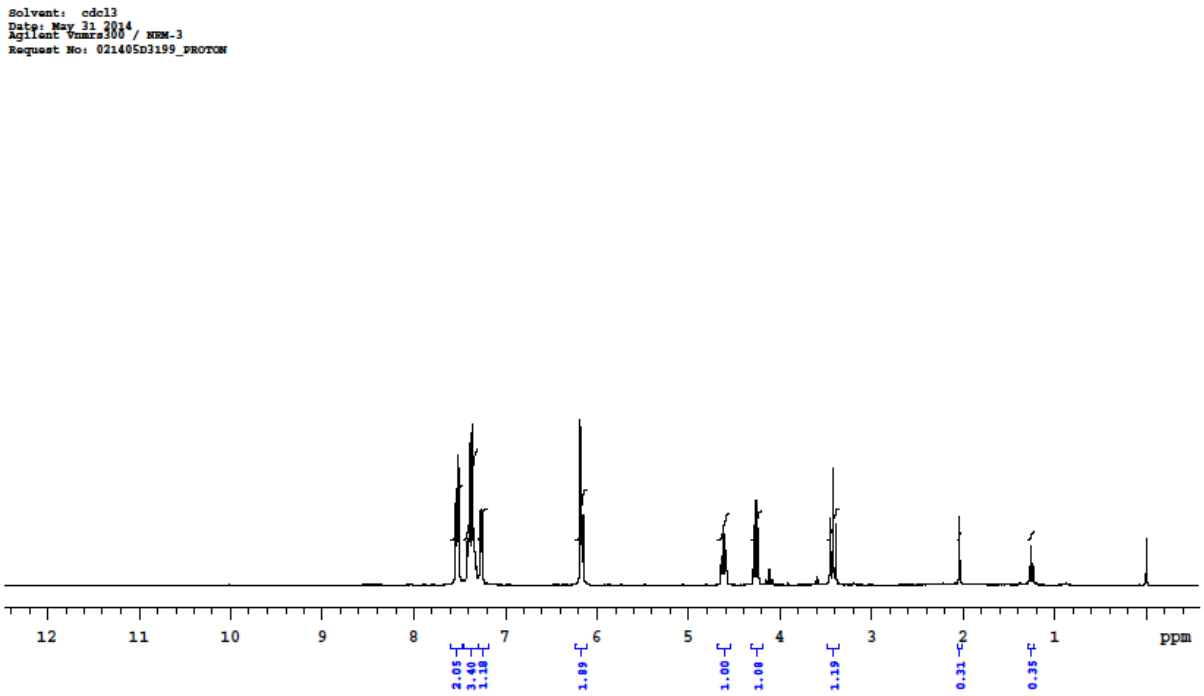
Solvent: cdcl3
Date: May 31 2014
Agilent Vnmrs300 / NRM-3
Request No: 021405D3199_PROTON
12
11
10
9
8
7
6
5
4
3
2
1
ppm
2.05
3.40
1.18
1.89
1.00
1.08
1.19
0.31
0.35

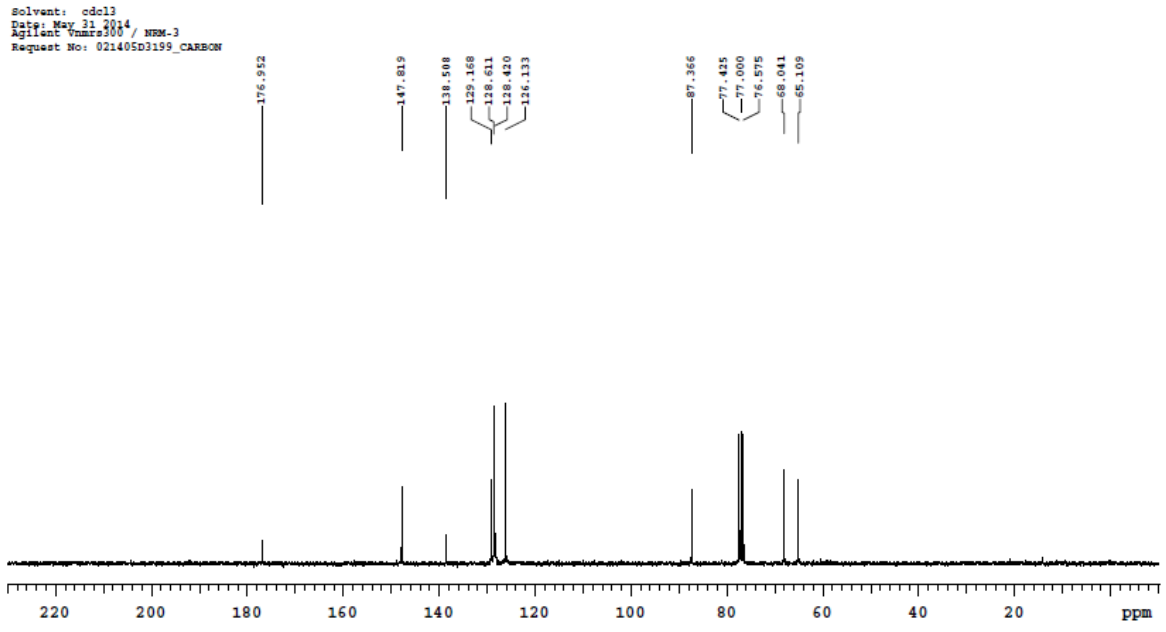
Solvent: cdcl3
Date: May 31 2014
Agilent Vnmrs300 / NRM-3
Request No: 021405D3199_CARBON
176.952
147.819
138.508
129.168
128.611
128.420
126.133
87.366
77.425
77.000
76.575
68.041
65.109
220
200
180
160
140
120
100
80
60
40
20
ppm

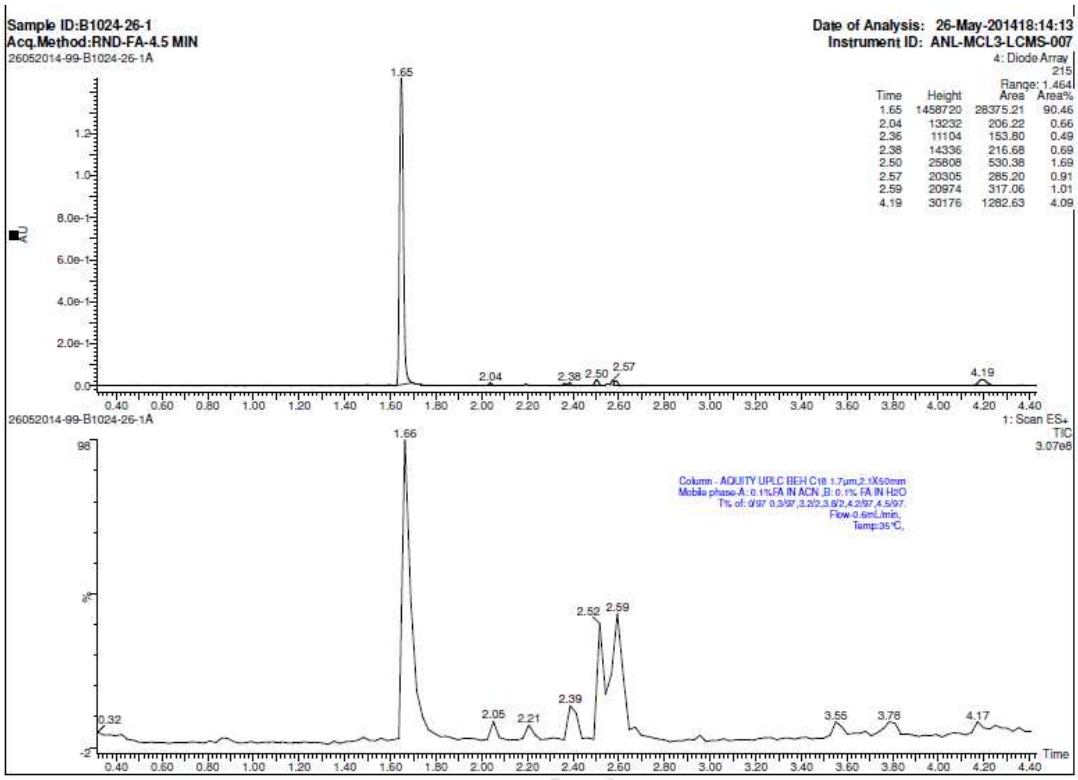
Sample ID:B1024-26-1
Acq.Method:RND-FA-4.5 MIN
26052014-99-B1024-26-1A
Date of Analysis: 26-May-201418:14:13
Instrument ID: ANL-MCL3-LCMS-007
4: Diode Array
215
Range: 1.464
Time Height Area Area%
1.65 1458720 28375.21 90.46
2.04 13232 206.22 0.66
2.36 11104 153.80 0.49
2.38 14336 216.68 0.69
2.50 25808 530.38 1.69
2.57 20305 285.20 0.91
2.59 20974 317.06 1.01
4.19 30176 1282.63 4.09
AU
1.65
2.04
2.38
2.50
2.57
4.19
26052014-99-B1024-26-1A
1: Scan ES+
TIC
3.07e8
1.66
Column - ACQUITY UPLC BEH C18 1.7µm,2.1X50mm
Mobile phase-A : 0.1%FA IN ACN ,B: 0.1% FA IN H2O
T% of: 0/97 0.3/97 ,3.2/2,3.8/2,4.2/97,4.5/97.
Flow-0.6mL/min,
Temp:35°C,
2.52
2.59
2.39
2.05
2.21
0.32
3.55
3.78
4.17
Time

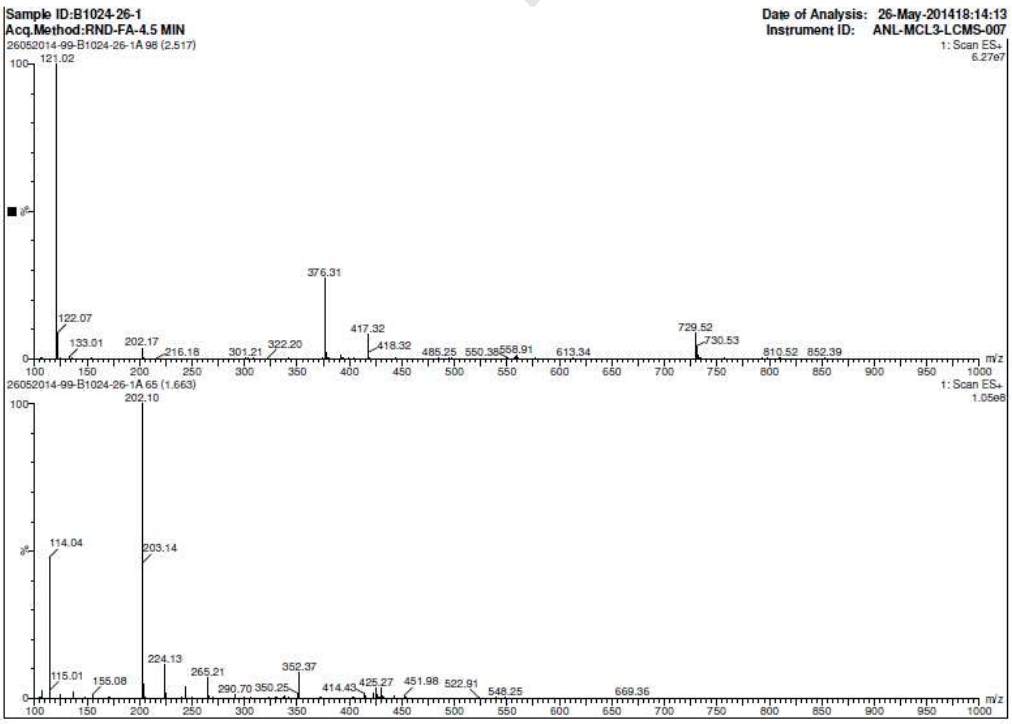
Sample ID:B1024-26-1
Acq.Method:RND-FA-4.5 MIN
Date of Analysis: 26-May-201418:14:13
Instrument ID: ANL-MCL3-LCMS-007
26052014-99-B1024-26-1A 98 (2.517)
1: Scan ES+
6.27e7
121.02
376.31
122.07
417.32
729.52
730.53
m/z
26052014-99-B1024-26-1A 65 (1.663)
1: Scan ES+
1.05e8
202.10
114.04
203.14
224.13
352.37
m/z

Compound **1**

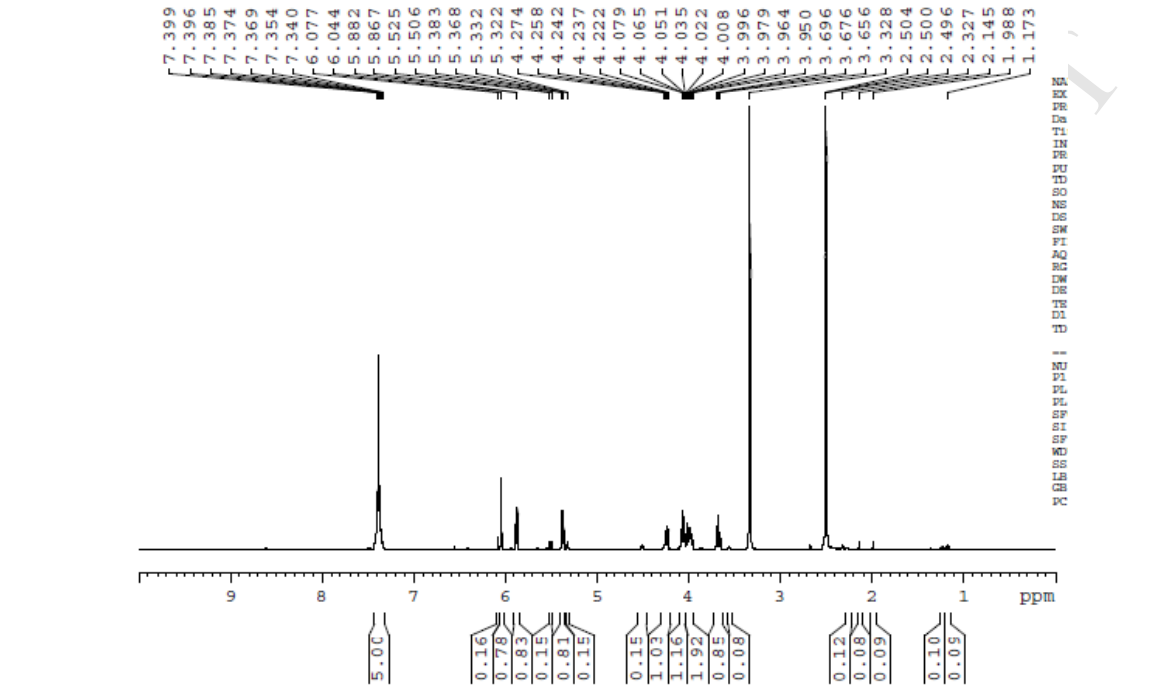
7.399
7.396
7.385
7.374
7.369
7.354
7.340
6.077
6.044
5.882
5.867
5.525
5.506
5.383
5.368
5.332
5.322
4.274
4.258
4.242
4.237
4.222
4.079
4.065
4.051
4.035
4.022
4.008
3.996
3.979
3.964
3.950
3.696
3.676
3.656
3.328
2.504
2.500
2.496
2.327
2.145
1.988
1.173
9
8
7
6
5
4
3
2
1
ppm
5.00
0.16
0.78
0.83
0.15
0.81
0.15
0.15
1.03
1.16
1.92
0.85
0.08
0.12
0.08
0.09
0.10
0.09

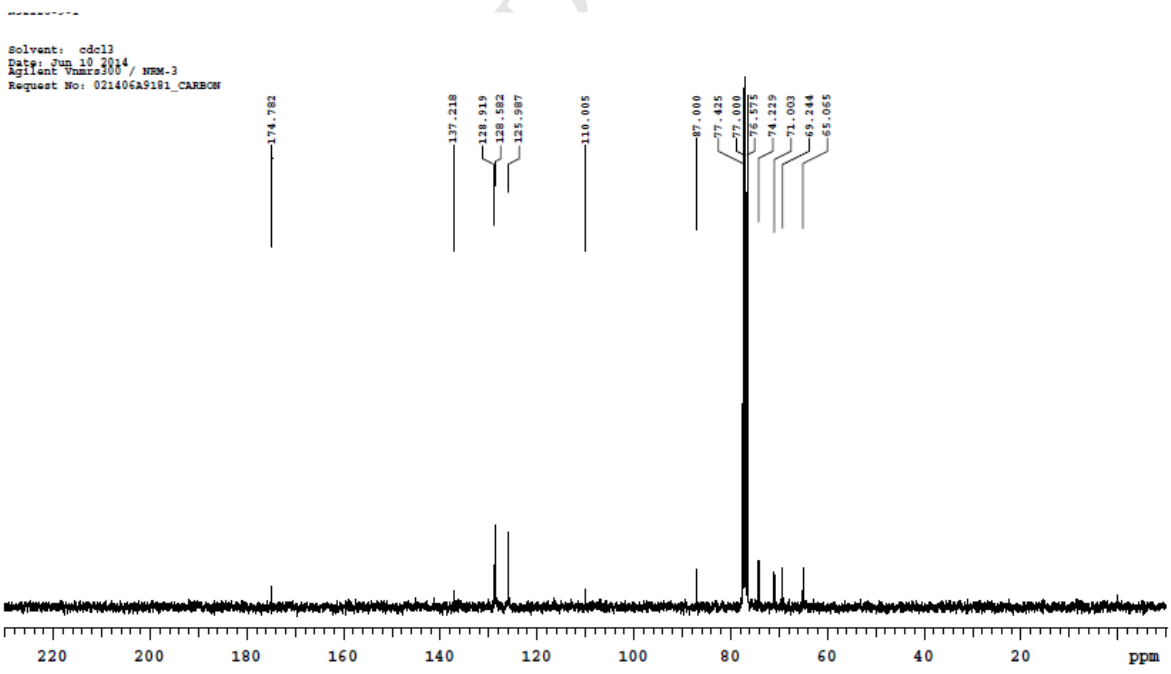
Solvent: cdcl3
Date: Jun 10 2014
Agilent Vnmrs500 / NRM-3
Request No: 021406A9181_CARBON
174.782
137.218
128.919
128.582
125.987
110.005
87.000
77.425
77.000
76.575
74.229
71.003
69.244
65.065
220
200
180
160
140
120
100
80
60
40
20
ppm

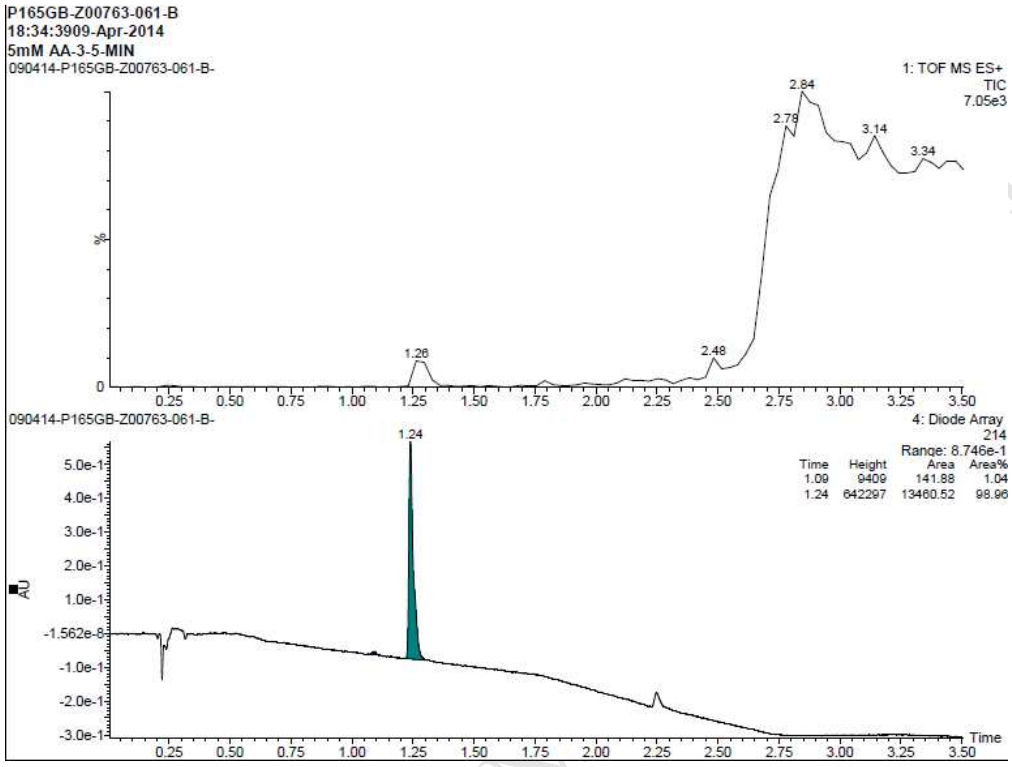

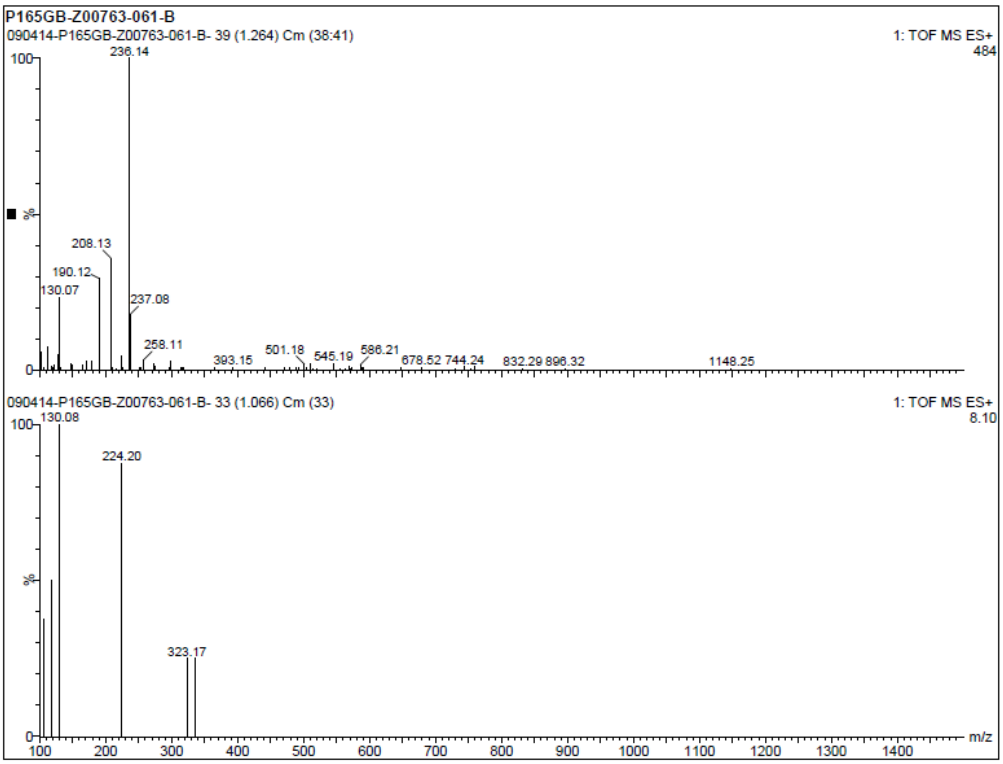

Compound 7

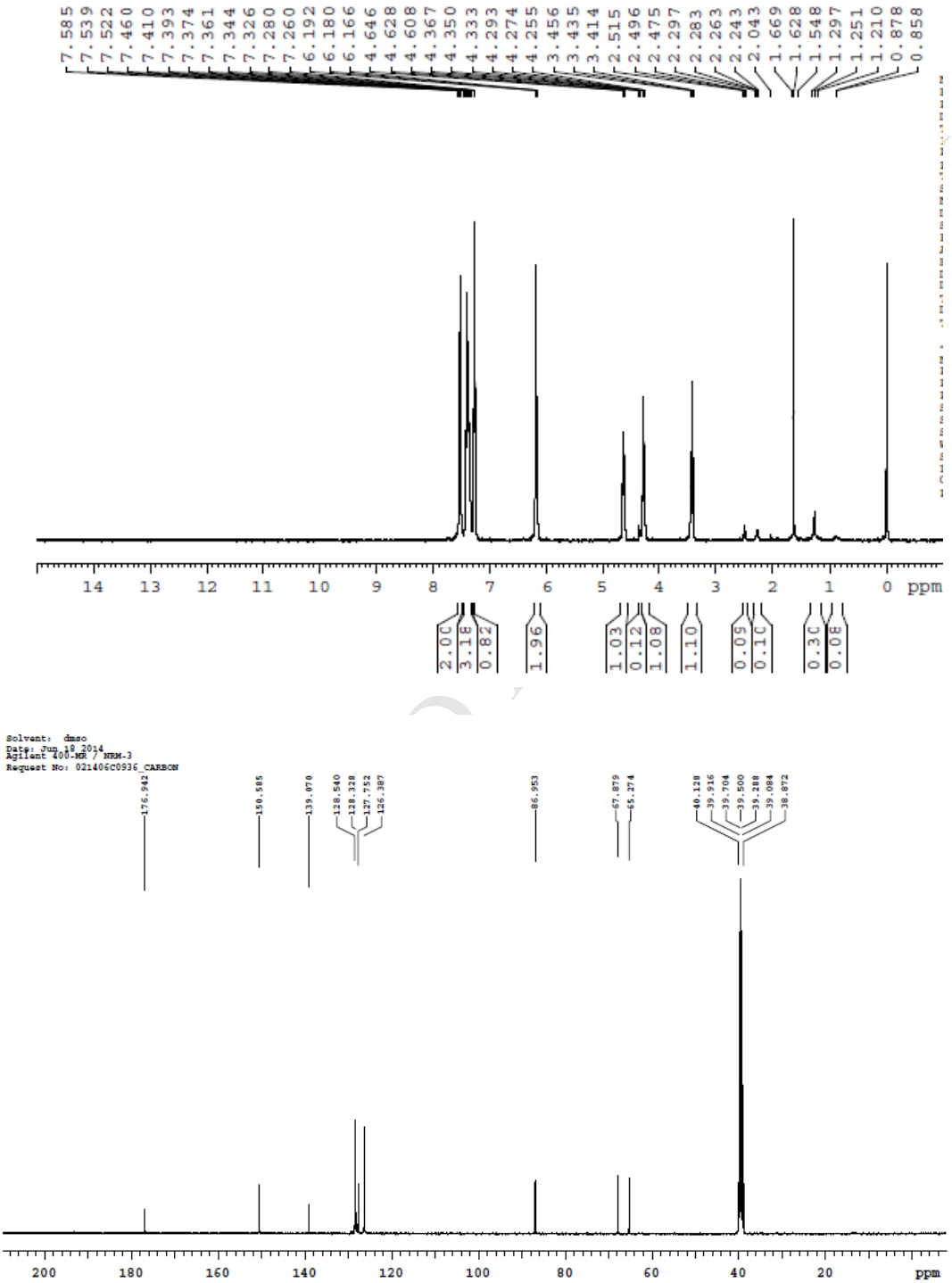
7.585
7.539
7.522
7.460
7.410
7.393
7.374
7.361
7.344
7.326
7.280
7.260
6.192
6.180
6.166
4.646
4.628
4.608
4.367
4.350
4.333
4.293
4.274
4.255
3.456
3.435
3.414
2.515
2.496
2.475
2.297
2.283
2.263
2.243
2.043
1.669
1.628
1.548
1.297
1.251
1.210
0.878
0.858
14 13 12 11 10 9 8 7 6 5 4 3 2 1 0 ppm
2.00
3.18
0.82
1.96
1.03
0.12
1.08
1.10
0.09
0.10
0.30
0.08
Solvent: dmso
Date: Jun 18 2014
Agilent 400-MR 7 MRM-3
Request No: 021406C0936_CARBON
176.942
150.585
139.070
128.540
128.328
127.752
126.387
86.953
67.879
65.274
40.128
39.916
39.704
39.500
39.288
39.084
38.872
200 180 160 140 120 100 80 60 40 20 ppm

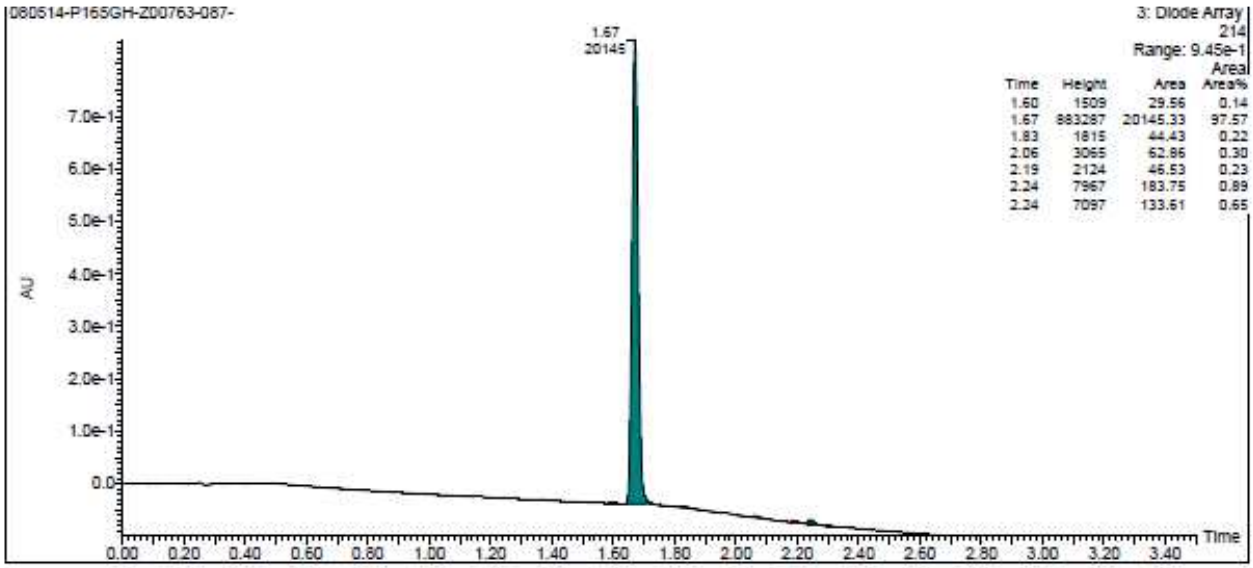
080514-P165GH-Z00763-087-
3: Diode Array
214
Range: 9.45e-1
1.67
20145
Time Height Area Area%
1.60 1509 29.56 0.14
1.67 883287 20145.33 97.57
1.83 1815 44.43 0.22
2.06 3065 62.86 0.30
2.19 2124 46.53 0.23
2.24 7967 183.75 0.89
2.24 7097 133.61 0.65
AU
Time

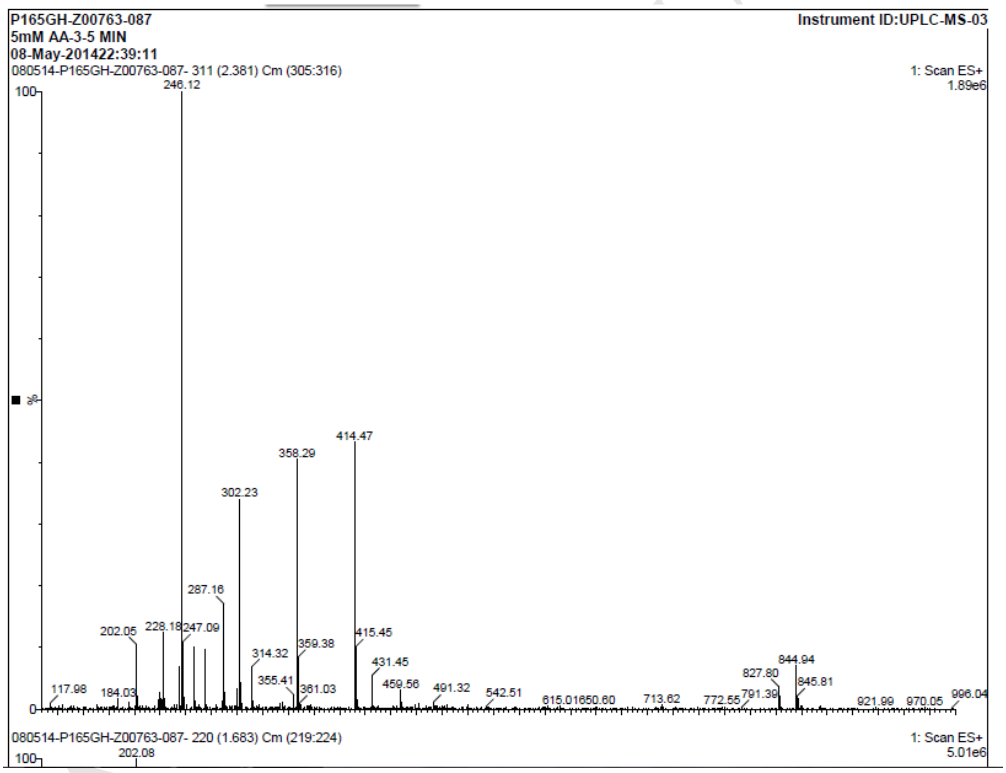
P165GH-Z00763-087
5mM AA-3-5 MIN
08-May-201422:39:11
Instrument ID:UPLC-MS-03
080514-P165GH-Z00763-087- 311 (2.381) Cm (305:316)
1: Scan ES+
1.89e6
246.12
414.47
358.29
302.23
287.16
202.05
228.18
247.09
359.38
415.45
314.32
431.45
355.41
361.03
459.56
491.32
542.51
844.94
827.80
845.81
117.98
184.03
615.01650.60
713.62
772.55
791.39
921.99
970.05
996.04
080514-P165GH-Z00763-087- 220 (1.683) Cm (219:224)
1: Scan ES+
5.01e6
202.08

Compound **8**

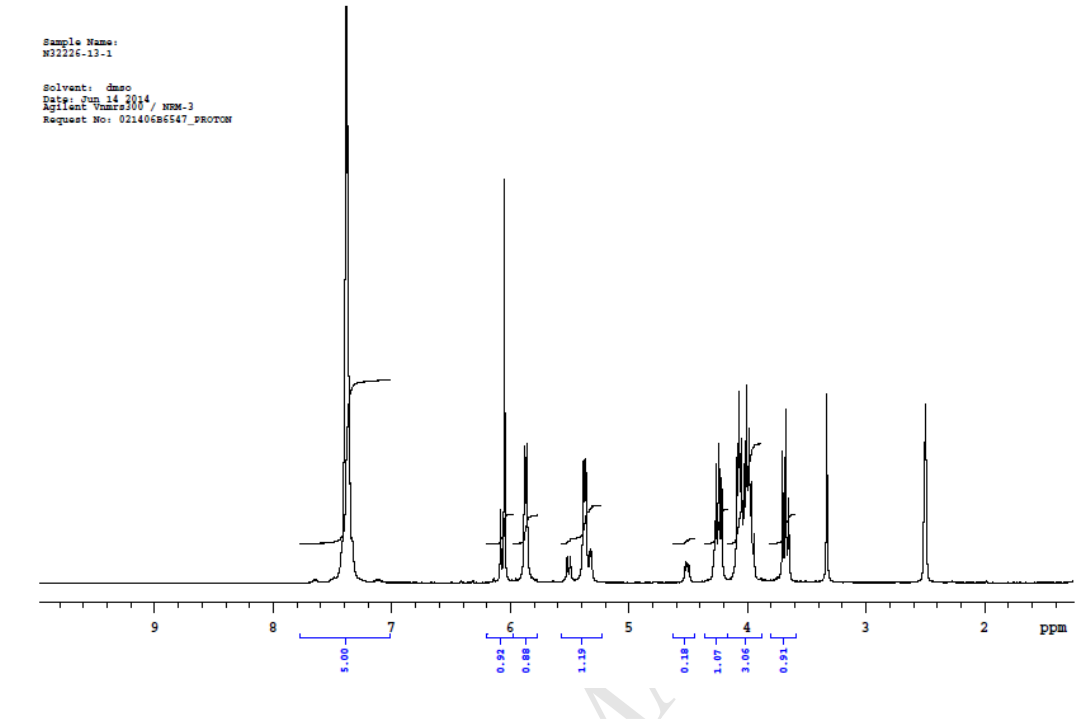
Sample Name:
N32226-13-1
Solvent: dmso
Date: Jun 14 2014
Agilent Vnmrs300 / NRM-3
Request No: 021406B6547_PROTON
9
8
7
6
5
4
3
2
ppm
5.00
0.92
0.88
1.19
0.18
1.07
3.06
0.91

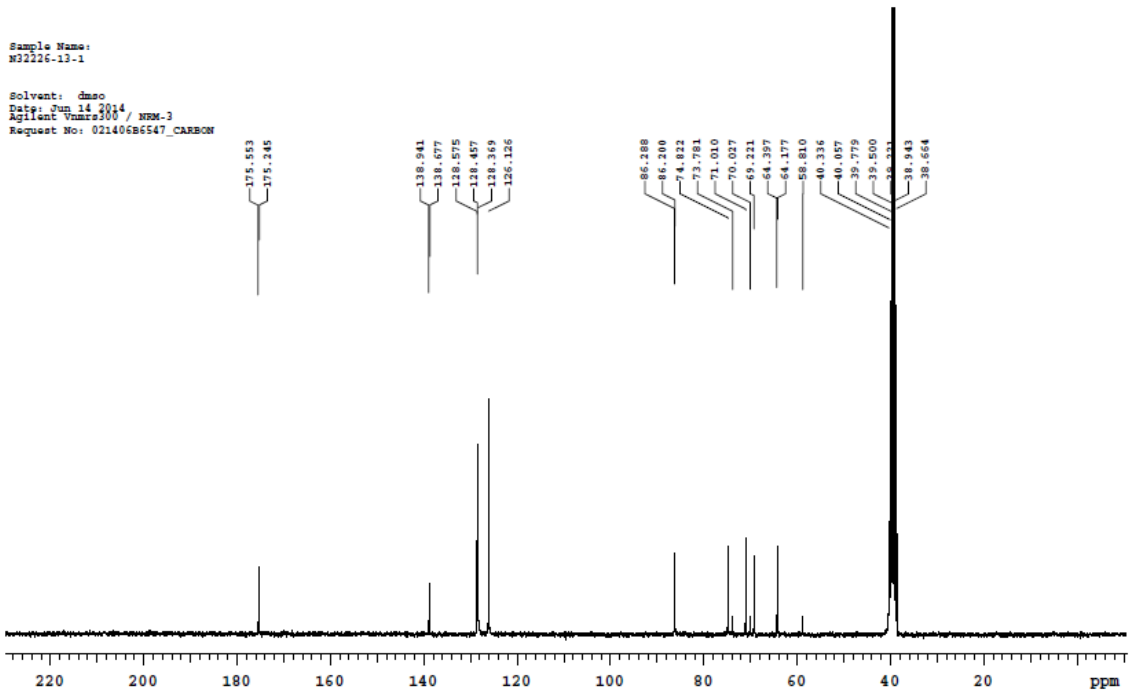
Sample Name:
N32226-13-1
Solvent: dmso
Date: Jun 14 2014
Agilent Vnmrs300 / NRM-3
Request No: 021406B6547_CARBON
175.553
175.245
138.941
138.677
128.575
128.457
128.369
126.126
86.288
86.200
74.822
73.781
71.010
70.027
69.221
64.397
64.177
58.810
40.336
40.057
39.779
39.500
38.943
38.664
220
200
180
160
140
120
100
80
60
40
20
ppm

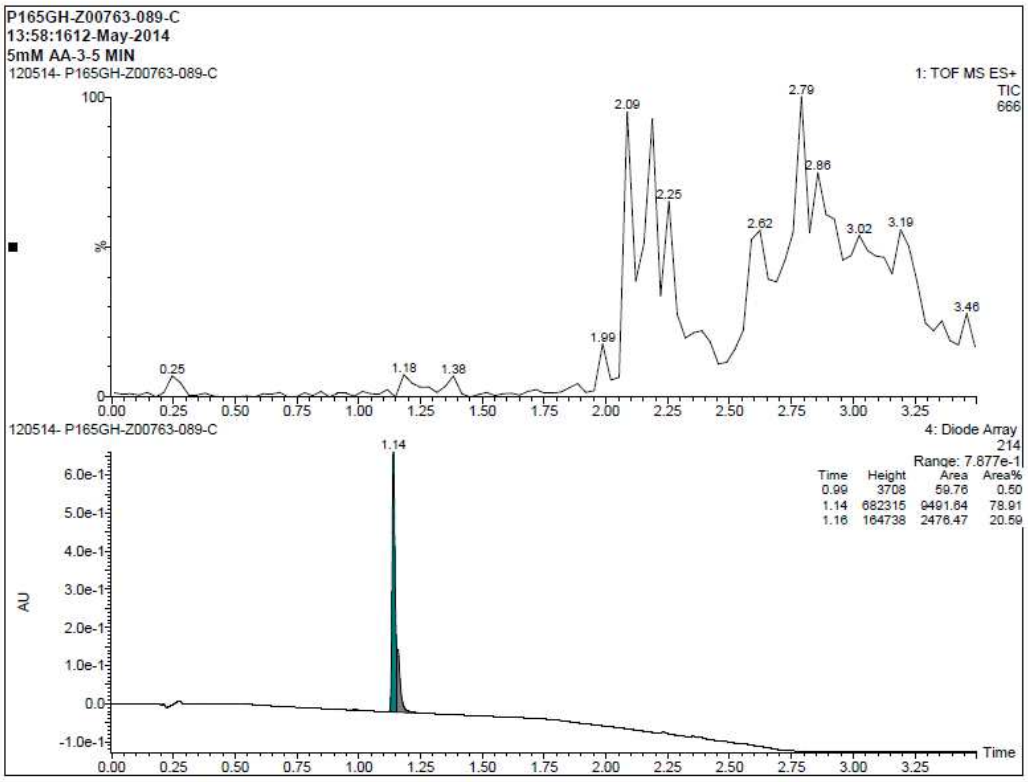
P165GH-Z00763-089-C
13:58:1612-May-2014
5mM AA-3-5 MIN
120514- P165GH-Z00763-089-C
1: TOF MS ES+
TIC
666
2.09
2.79
2.86
2.25
2.62
3.02
3.19
3.46
1.99
0.25
1.18
1.38
120514- P165GH-Z00763-089-C
4: Diode Array
214
Range: 7.877e-1
1.14
Time Height Area Area%
0.99 3708 59.76 0.50
1.14 682315 9491.64 78.91
1.16 164738 2476.47 20.59
AU
Time

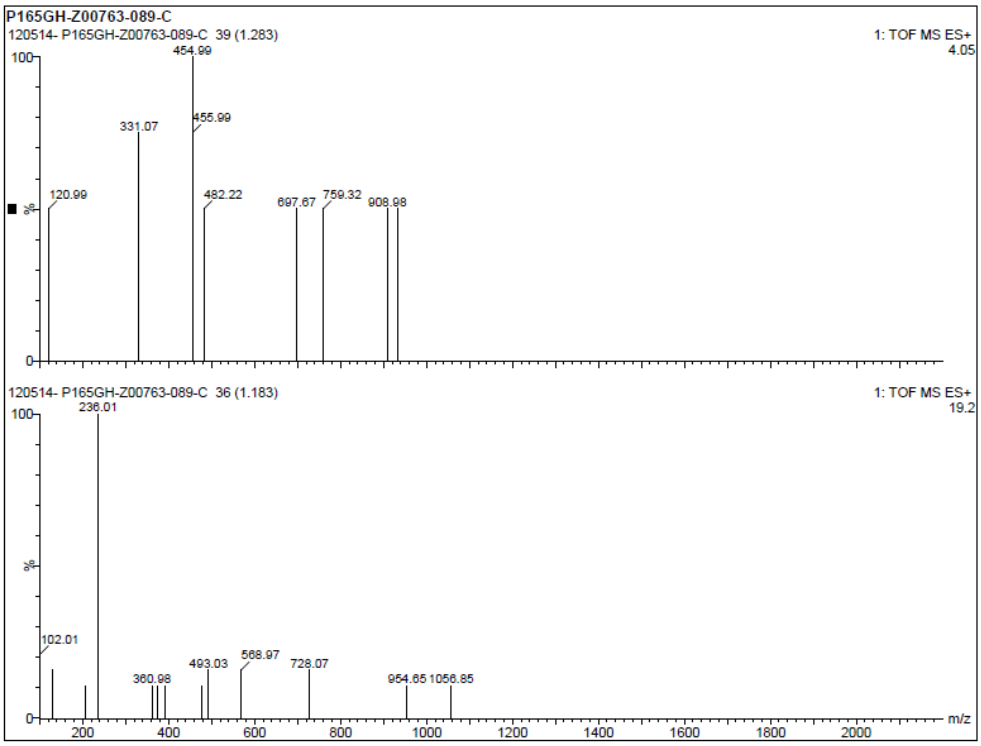
P165GH-Z00763-089-C
120514- P165GH-Z00763-089-C 39 (1.283)
1: TOF MS ES+
4.05
454.99
455.99
331.07
120.99
482.22
697.67
759.32
908.98
120514- P165GH-Z00763-089-C 36 (1.183)
1: TOF MS ES+
19.2
236.01
102.01
360.98
493.03
568.97
728.07
954.65
1056.85
m/z

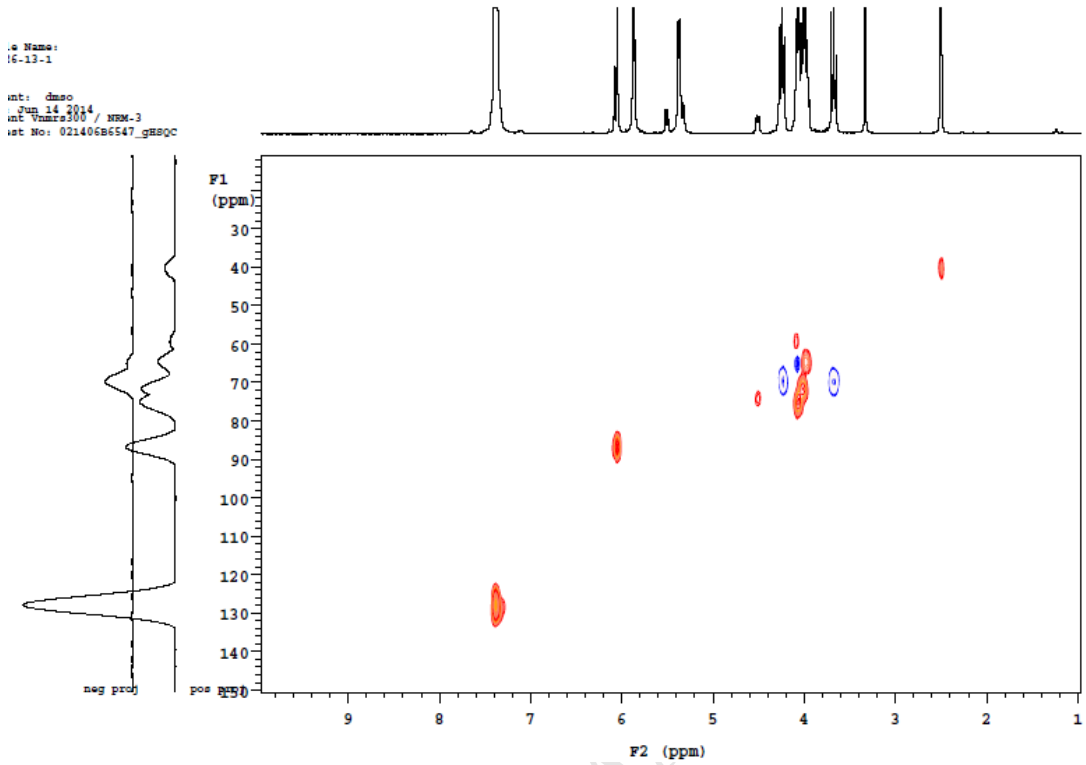
F1
(ppm)
F2 (ppm)
neg proj
pos proj

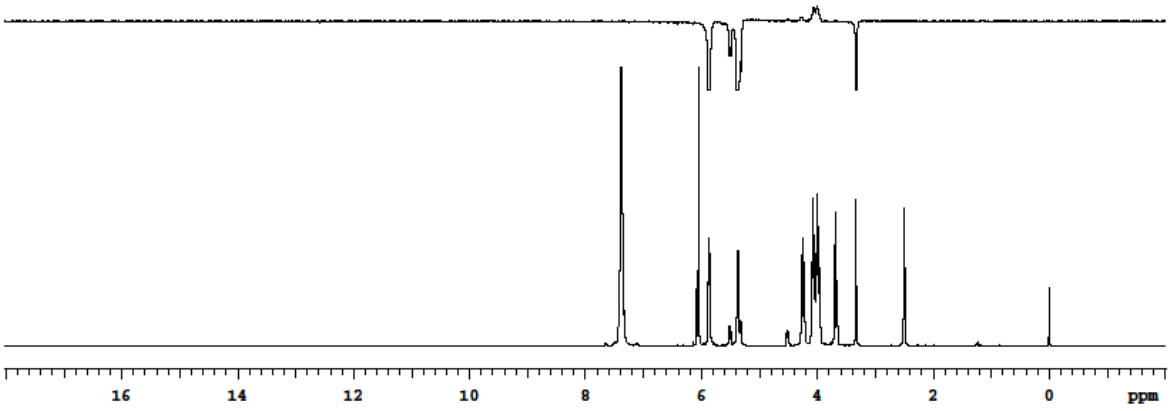
ppm

Compound **12**

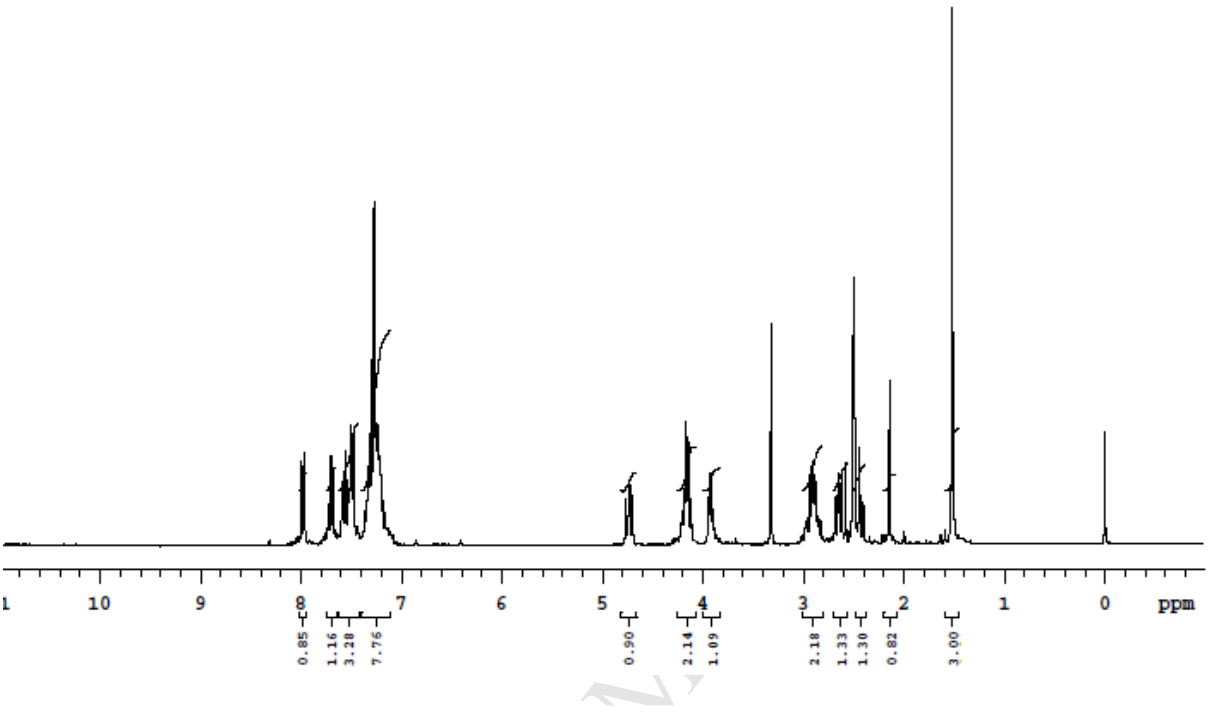
10
9
8
7
6
5
4
3
2
1
0
ppm
0.85
1.16
3.28
7.76
0.90
2.14
1.09
2.18
1.33
1.30
0.82
3.00

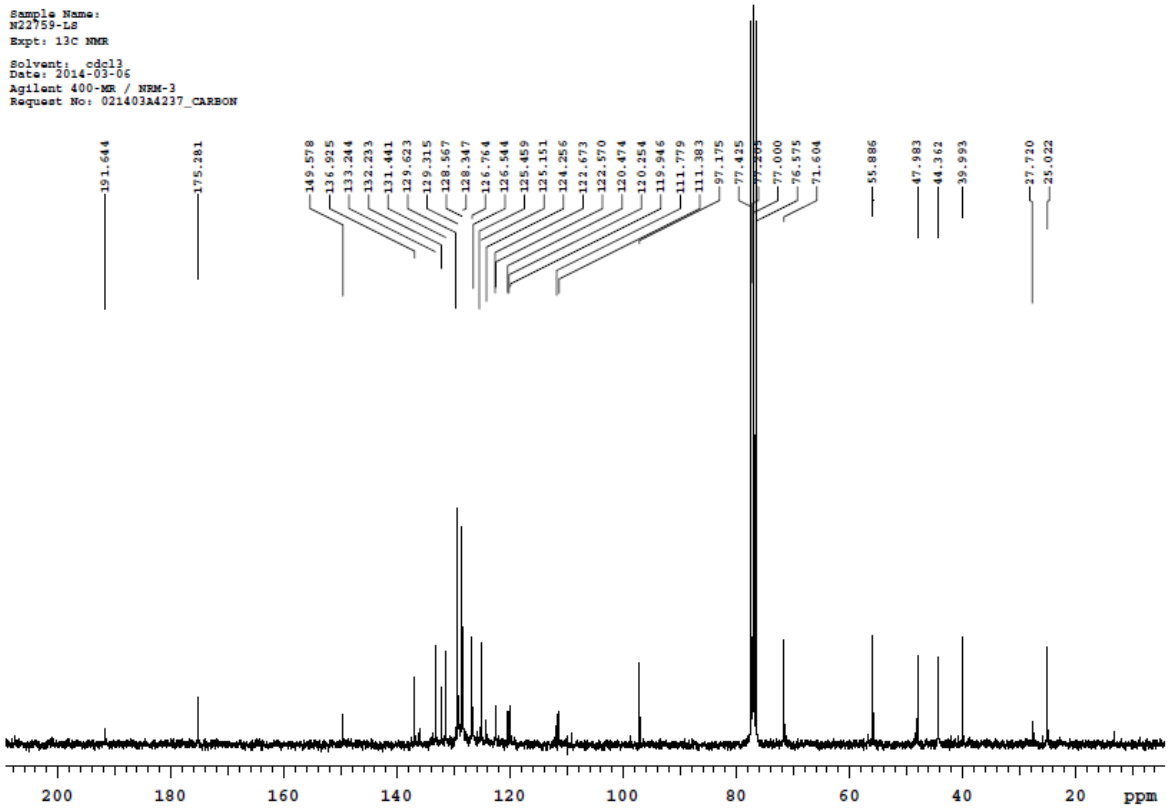
Sample Name:
N22759-LS
Expt: 13C NMR
Solvent: cdcl3
Date: 2014-03-06
Agilent 400-MR / NRM-3
Request No: 021403A4237_CARBON
191.644
175.281
149.578
136.925
133.244
132.233
131.441
129.623
129.315
128.567
128.347
126.764
126.544
125.459
125.151
124.256
122.673
122.570
120.474
120.254
119.946
111.779
111.383
97.175
77.425
77.000
76.575
71.604
55.886
47.983
44.362
39.993
27.720
25.022
200
180
160
140
120
100
80
60
40
20
ppm

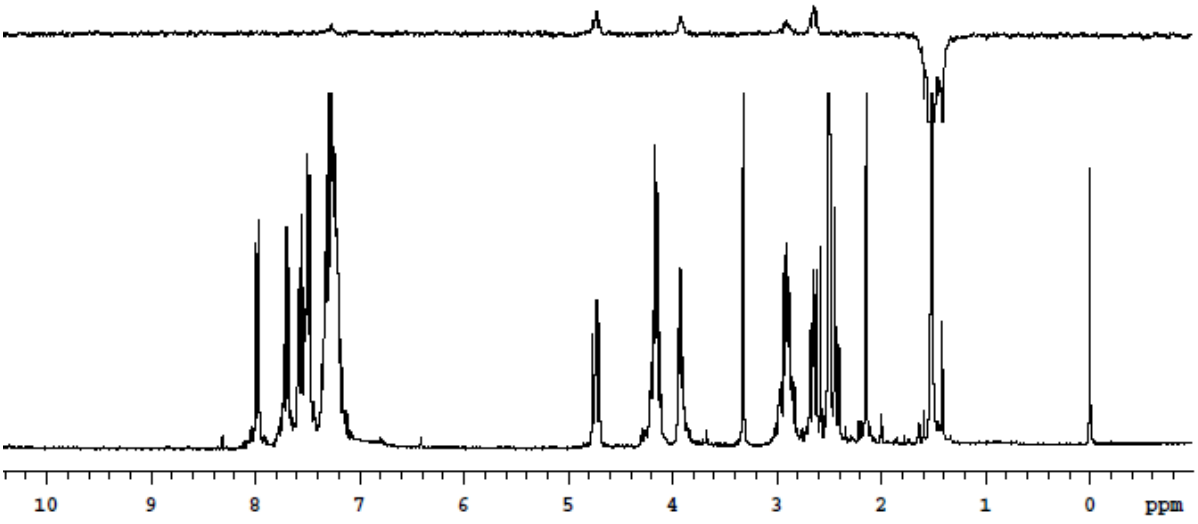
10
9
8
7
6
5
4
3
2
1
0
ppm

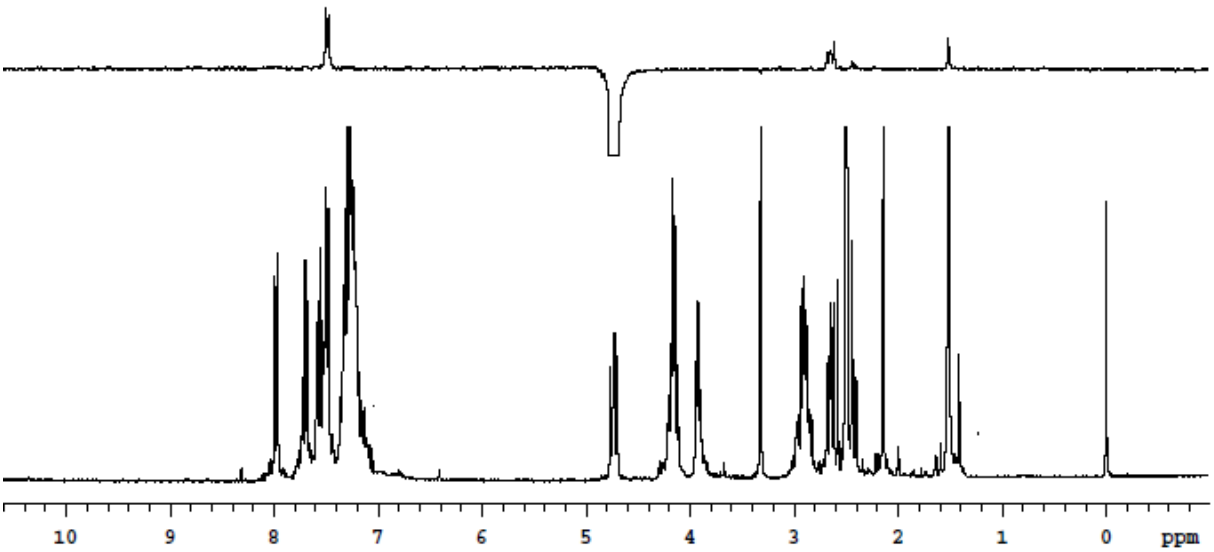
10
9
8
7
6
5
4
3
2
1
0
ppm

Compound **13**

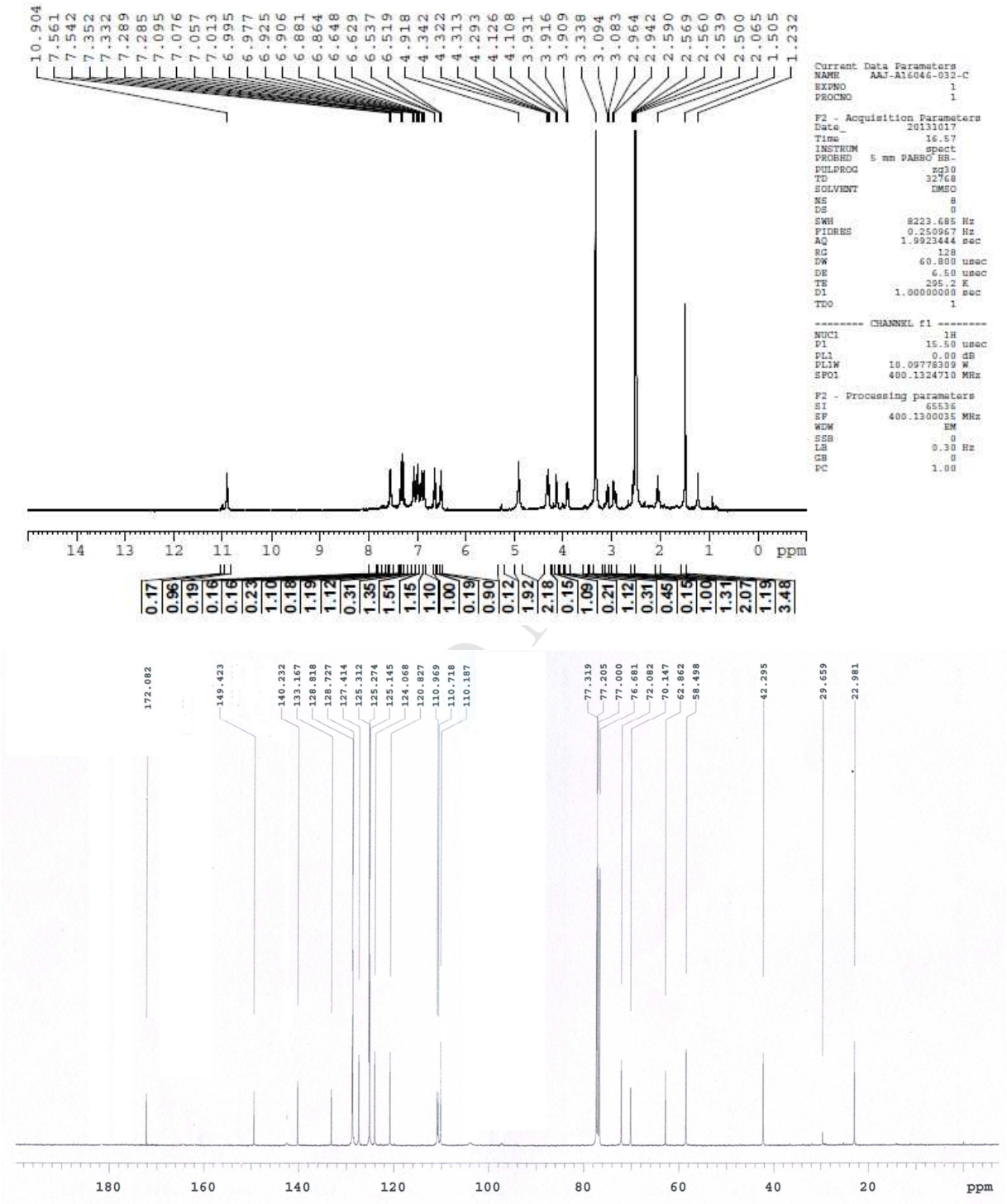
10.904
7.561
7.542
7.352
7.332
7.289
7.285
7.095
7.076
7.057
7.013
6.995
6.977
6.925
6.906
6.881
6.864
6.648
6.629
6.537
6.519
4.918
4.342
4.322
4.313
4.293
4.126
4.108
3.931
3.916
3.909
3.338
3.094
3.083
2.964
2.942
2.590
2.569
2.560
2.539
2.500
2.065
1.505
1.232
Current Data Parameters
NAME AAJ-A16046-032-C
EXPNO 1
PROCNO 1
F2 - Acquisition Parameters
Date_ 20131017
Time 16.57
INSTRUM spect
PROBHD 5 mm PABBO BB-
PULPROG zg30
TD 32768
SOLVENT DMSO
NS 8
DS 0
SWH 8223.685 Hz
FIDRES 0.250967 Hz
AQ 1.9923444 sec
RG 128
DW 60.800 usec
DE 6.50 usec
TE 295.2 K
D1 1.00000000 sec
TD0 1
-------- CHANNEL f1 --------
NUC1 1H
P1 15.50 usec
PL1 0.00 dB
PL1W 10.09778309 W
SFO1 400.1324710 MHz
F2 - Processing parameters
SI 65536
SF 400.1300035 MHz
WDW EM
SSB 0
LB 0.30 Hz
GB 0
PC 1.00
14 13 12 11 10 9 8 7 6 5 4 3 2 1 0 ppm
0.17 0.96 0.19 0.16 0.16 0.23 1.10 0.18 1.19 1.12 0.31 1.35 1.51 1.15 1.10 1.00 0.19 0.90 0.12 1.92 2.18 0.15 1.09 0.21 1.12 0.31 0.45 0.15 1.00 1.31 2.07 1.19 3.48
172.082
149.423
140.232
133.167
128.818
128.727
127.414
125.312
125.274
125.145
124.068
120.827
110.969
110.718
110.187
77.319
77.205
77.000
76.681
72.082
70.147
62.862
58.498
42.295
29.659
22.981
180 160 140 120 100 80 60 40 20 ppm

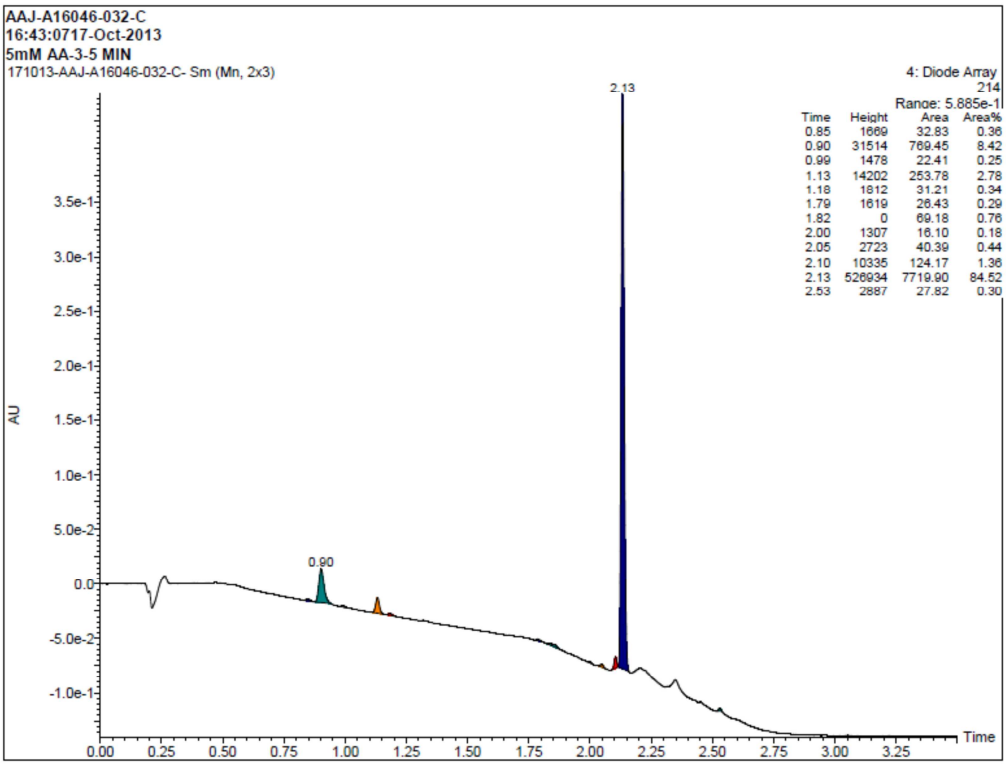

Compound **14**

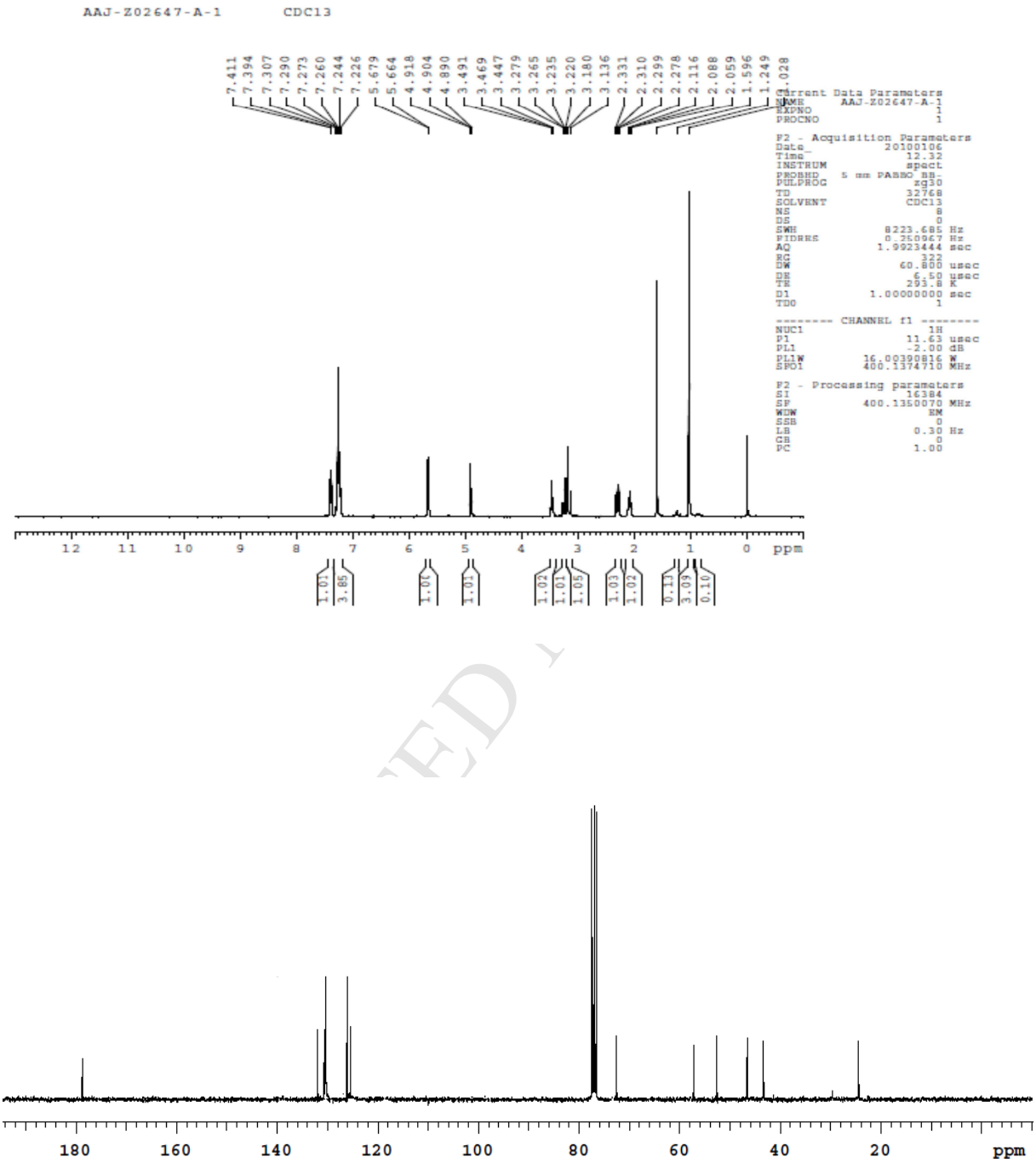
AAJ-Z02647-A-1 CDC13
7.411
7.394
7.307
7.290
7.273
7.260
7.244
7.226
5.679
5.664
4.918
4.904
4.890
3.491
3.469
3.447
3.279
3.265
3.235
3.220
3.180
3.136
2.331
2.310
2.299
2.278
2.116
2.088
2.059
1.596
1.249
0.028
Current Data Parameters
NAME AAJ-Z02647-A-1
EXPNO 1
PROCNO 1
F2 - Acquisition Parameters
Date_ 20100106
Time 12.32
INSTRUM spect
PROBHD 5 mm PABBO BB-
PULPROG zg30
TD 32768
SOLVENT CDC13
NS 8
DS 0
SWH 8223.685 Hz
FIDRES 0.250967 Hz
AQ 1.9923444 sec
RG 322
DW 60.800 usec
DE 6.50 usec
TE 293.8 K
D1 1.00000000 sec
TD0 1
======== CHANNEL f1 ========
NUC1 1H
P1 11.63 usec
PL1 -2.00 dB
PL1W 16.09390816 W
SFO1 400.1374710 MHz
F2 - Processing parameters
SI 16384
SF 400.1350070 MHz
WDW EM
SSB 0
LB 0.30 Hz
GB 0
PC 1.00
12 11 10 9 8 7 6 5 4 3 2 1 0 ppm
1.01
3.85
1.01
1.01
1.02
1.01
1.05
1.03
1.02
0.13
3.09
0.10
180 160 140 120 100 80 60 40 20 ppm

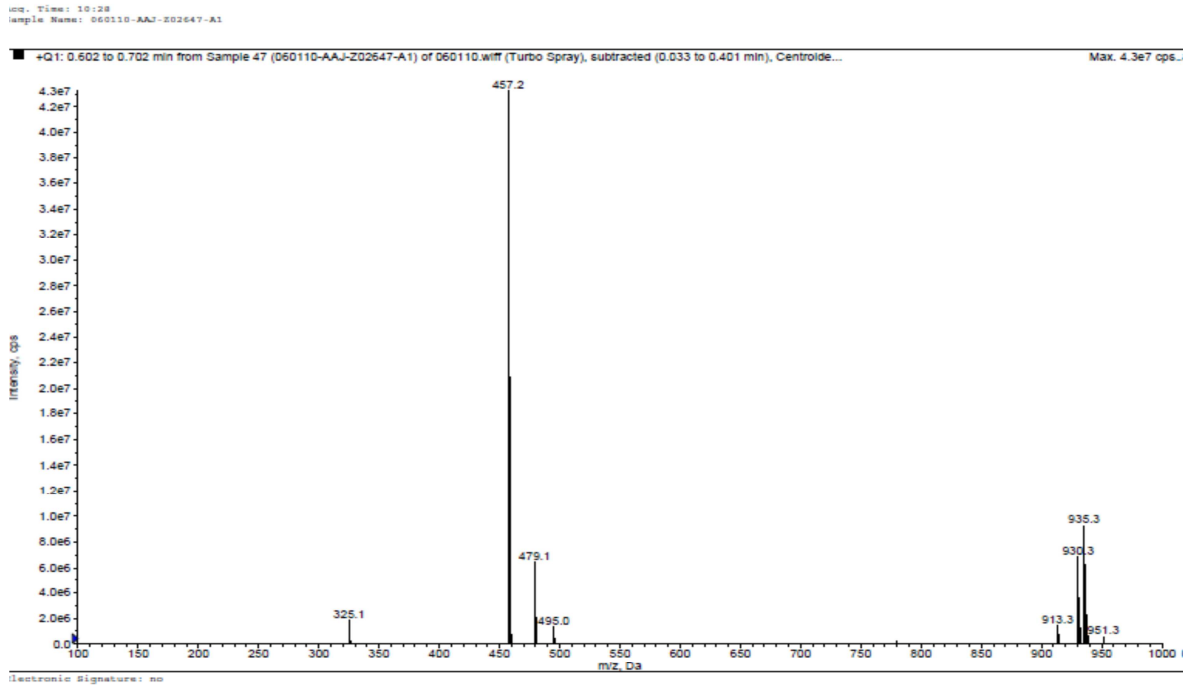

Compound **15**

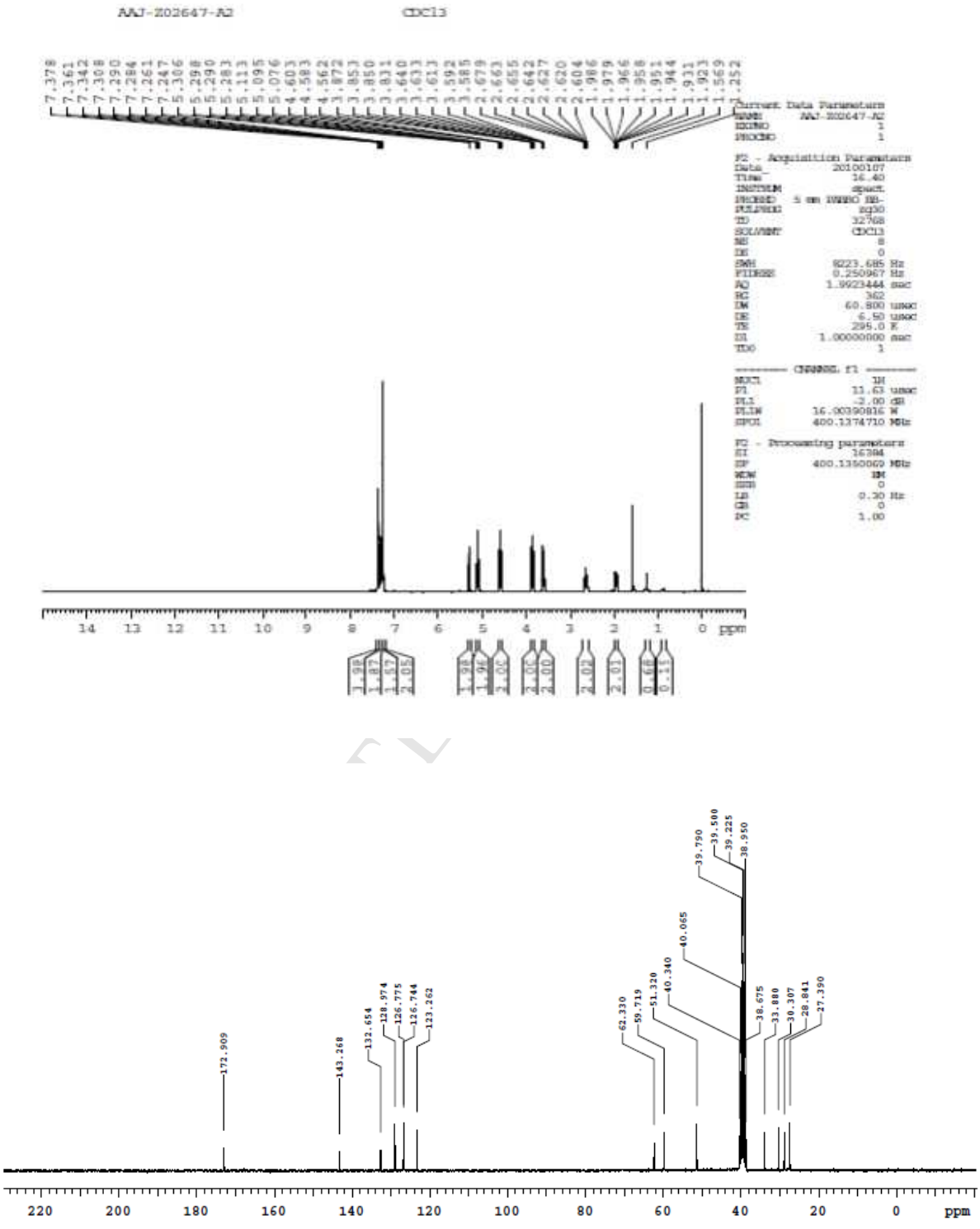
AAJ-Z02647-A2
CDCl3
7.378
7.361
7.342
7.308
7.290
7.284
7.261
7.247
5.306
5.298
5.290
5.283
5.113
5.095
5.076
4.603
4.583
4.562
3.872
3.853
3.850
3.831
3.640
3.633
3.613
3.592
3.585
3.579
2.663
2.655
2.642
2.627
2.620
2.604
1.986
1.979
1.966
1.958
1.951
1.944
1.931
1.923
1.569
1.252
Current Data Parameters
NAME AAJ-Z02647-A2
EXPNO 1
PROCNO 1
F2 - Acquisition Parameters
Date_ 20100107
Time 16.40
INSTRUM spect
PROBHD 5 mm PABBO BB-
PULPROG zg30
TD 32768
SOLVENT CDCl3
NS 8
DS 0
SWH 8223.685 Hz
FIDRES 0.250967 Hz
AQ 1.9923444 sec
RG 362
DW 60.800 usec
DE 6.50 usec
TE 295.0 K
D1 1.00000000 sec
TD0 1
CHANNEL f1
NUC1 1H
P1 11.63 usec
PL1 -2.00 dB
PLW1 16.00390816 W
SFO1 400.1374710 MHz
F2 - Processing parameters
SI 16384
SF 400.1350069 MHz
WDW EM
SSB 0
LB 0.30 Hz
GB 0
PC 1.00
14 13 12 11 10 9 8 7 6 5 4 3 2 1 0 ppm
1.98 1.87 1.67 2.05 1.98 1.94 3.00 2.00 2.00 2.02 2.01 0.66 0.41
172.909
143.268
132.654
128.974
126.775
126.744
123.262
62.330
59.719
51.320
40.340
40.065
39.790
39.500
39.225
38.950
38.675
33.880
30.307
28.841
27.390
220 200 180 160 140 120 100 80 60 40 20 0 ppm

Acq. Time: 15:36
Sample Name: 070110-AAJ-Z02647-A2

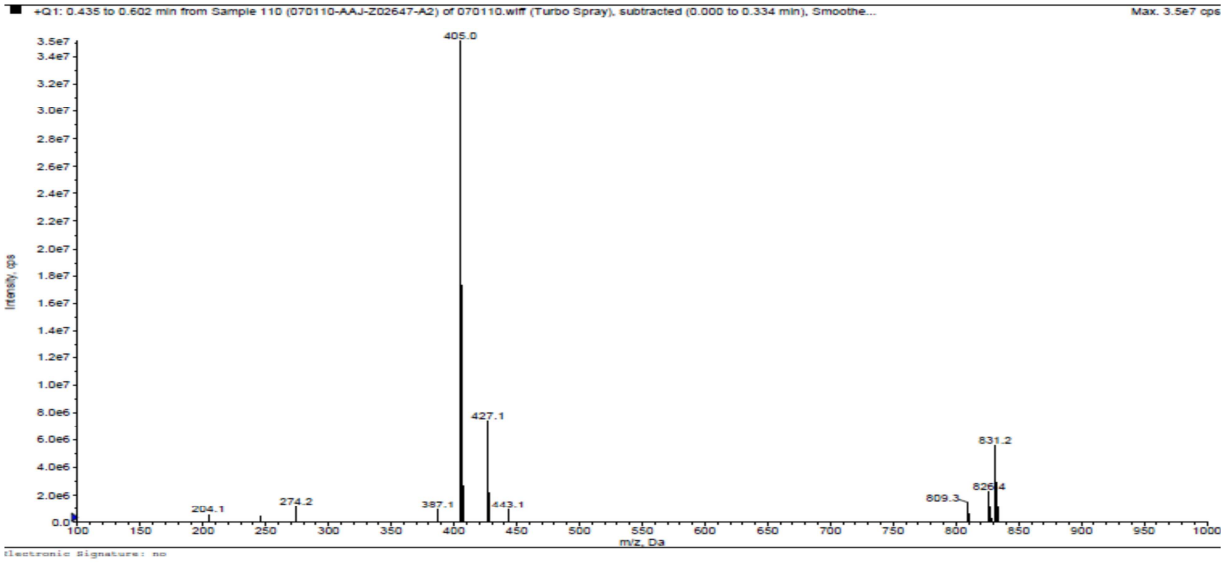

Electronic Signature: no

Compound **16**

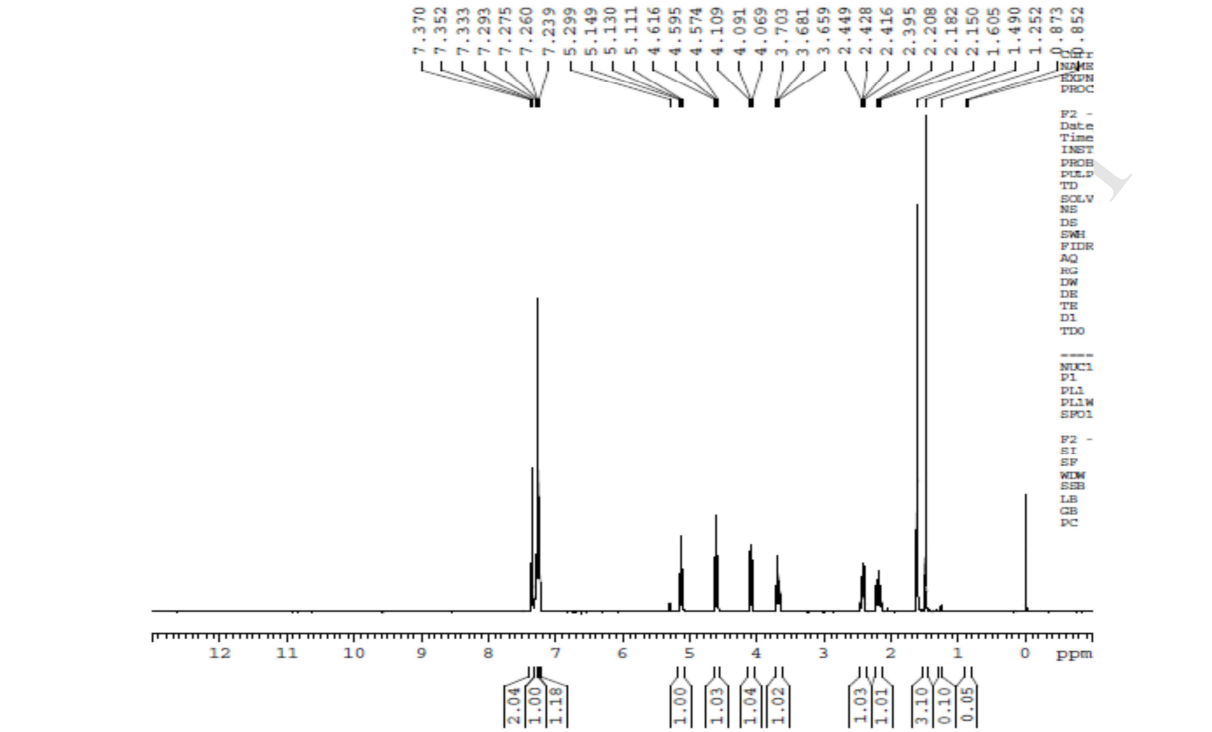
7.370
7.352
7.333
7.293
7.275
7.260
7.239
5.299
5.149
5.130
5.111
4.616
4.595
4.574
4.109
4.091
4.069
3.703
3.681
3.659
2.449
2.428
2.416
2.395
2.208
2.182
2.150
1.605
1.490
1.252
0.873
0.852
12
11
10
9
8
7
6
5
4
3
2
1
0
ppm
2.04
1.00
1.18
1.00
1.03
1.04
1.02
1.03
1.01
3.10
0.10
0.05

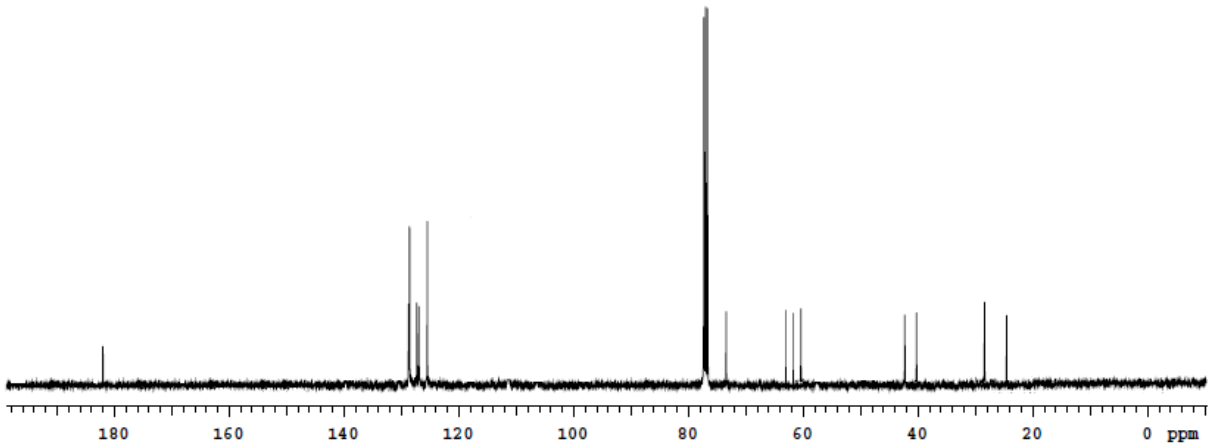
180
160
140
120
100
80
60
40
20
0
ppm

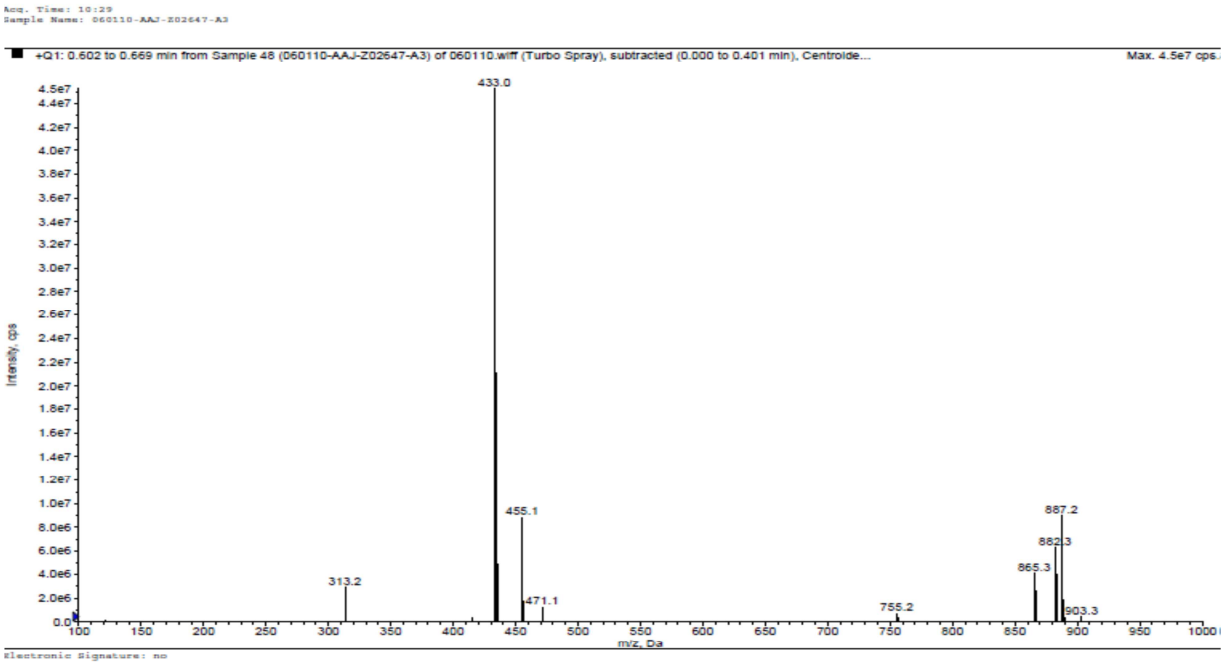

Compound **17**

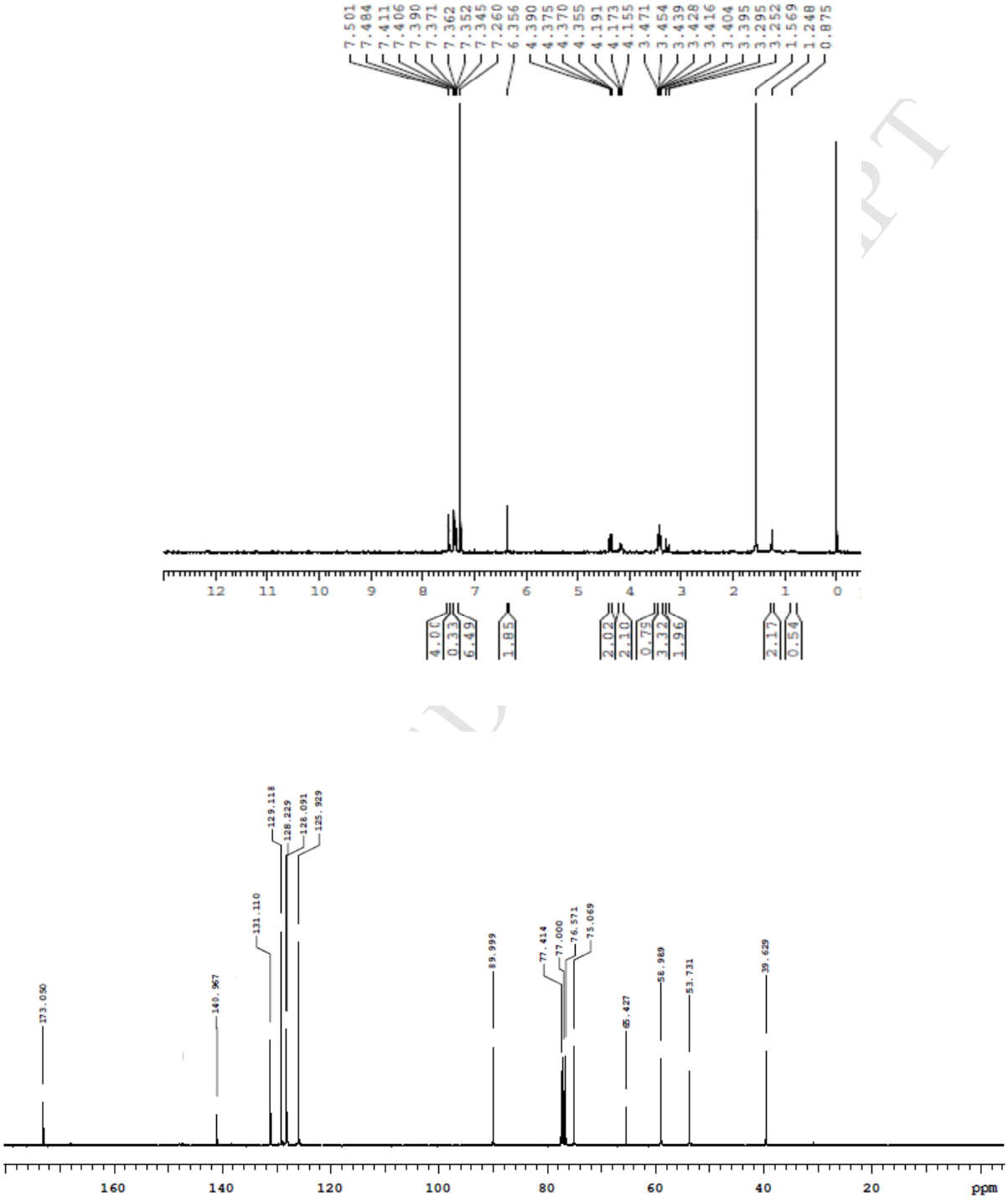
7.501
7.484
7.411
7.406
7.390
7.371
7.362
7.352
7.345
7.260
6.356
4.390
4.375
4.370
4.355
4.191
4.173
4.155
3.471
3.454
3.439
3.428
3.416
3.404
3.395
3.295
3.252
1.569
1.248
0.875
12 11 10 9 8 7 6 5 4 3 2 1 0
4.00
0.33
6.49
1.85
2.02
2.10
0.79
3.32
1.96
2.17
0.54
173.050
140.967
131.110
129.118
128.229
128.091
125.929
89.999
77.414
77.000
76.571
75.069
65.427
58.989
53.731
39.629
160 140 120 100 80 60 40 20 ppm